MEDIZINISCHE UNIVERSITÄT WIEN

Universität für Bodenkultur Wien
University of Natural Resources and Applied Life Sciences, Vienna

Master thesis

Alteration in lysosomal function and cyclin B1 expression as resistance mechanisms against T-DM1 in HER2 positive breast cancer models

for acquisition of the academic degree
Diplom- Ingenieurin (Dipl.-Ing.in)
on the University of Natural Resources and Applied Life Sciences, Vienna
by

Manuela Maria Warmuth, BSc.

October, 2019

SUPERVISED BY

Ao. Univ.-Prof. Dipl.- Ing. Dr. Florian Rüker

Ao. Univ.-Prof. Dipl.- Ing. Dr. Robert Mader

I hereby declare that I am the sole author of this work. No assistance other than that which is permitted has been used. Ideas and quotes taken directly or indirectly from other sources are identified as such. This written work has not yet been submitted in any part.

……..

Manuela Warmuth

Vienna, 16.10.2019

Acknowledgements

I would first like to thank Prof. Robert Mader for giving me the opportunity to conduct my master thesis in his research group at the MedUni Vienna and for providing a great support throughout my thesis.

I would also like to thank my supervisor Prof. Florian Rüker from the University of Natural Resources and Applied Life Sciences for the patient guidance, encouragement and advice he has provided me.

I have been extremely lucky to have two supervisors who cared so much about my work, and who responded to my questions and queries so promptly.

Additionally, I want to thank the entire research group for the positive and welcoming working atmosphere throughout the months I have spent at the laboratory, who always were happy to help in any given situation that I encountered. A special thanks for this goes to Birgit and Maria.

Finally, I must express my very profound gratitude to my parents and to my grandparents for providing me with unfailing support and continuous encouragement throughout my years of study and through the process of researching and writing this thesis. This accomplishment would not have been possible without them. Thank you.

Abstract

Breast cancer is one of the most common cancer types in women worldwide. 15-20% of the breast cancer patients suffer from the HER2/neu positive primary breast cancer type; this aggressive cancer form has a genetic amplification leading to an overexpression of the HER2 protein. Trastuzumab is used as first line therapy while trastuzumab emtansine (T-DM1) is a standard treatment used as second line therapy in advanced HER2-positive metastatic breast cancer. T-DM1 consists of the monoclonal antibody trastuzumab coupled with a cytotoxic agent which was originally isolated from the Ethiopian shrub Maytenus serrata. However, most patients develop resistance to T-DM1 within one year. Several resistance mechanisms are suspected but only a few have been researched so far. In this work, two of these putative resistance mechanisms were described in more detail: a change of the lysosomal function as well as an aberrant cyclinB1/Cdk1 expression. To confirm an alteration in lysosomal function, the pH in the lysosomes as examined by pHrodo staining was found to be increased in the resistant cell lines. However, increasing the lysosomal pH using chloroquine alone and combination with T-DM1 was hard to interpret in cytotoxicity testing due to the high variability of the results, probably caused by the inherent toxicity of chloroquine itself. In addition to the lysosomal pH increase in resistance, there was an increase in lysosome counts per cell with increasing resistance to T-DM1. The cathepsin expression, the T-DM1 cleaving enzyme, had little influence on resistance. Another candidate, the cyclinB1/CdK1 complex might also be crucial for the action of T-DM1, since DM1 acts only in the M phase of the cell, where spindle assembly is disturbed by T-DM1. However, our hypothesis that an aberrant complex leads to cell resistance could be refuted by various experiments. On the contrary, cyclinB1 expression even increased with increasing resistance levels, which also coincides with the shorter generation time of resistant cells compared to their sensitive mother cell line. Interestingly, T-DM1 resistance had no impact on DNA synthesis as shown by BrdU assays. Upon exposure to T-DM1, cyclinB1 expression increased in both the sensitive and the resistant subclones. In conclusion, an aberrant expression of cyclinB1 has no direct influence on T-DM1 resistance, but it can be stated that the antibody-drug conjugates lead to an accumulation of cyclinB1 in all cell lines. In contrast, an altered lysosomal pH could

be confirmed as a possible resistance mechanism, which was associated with a higher lysosome count in resistant cell lines.

Zusammenfassung

Brustkrebs ist eine der häufigsten Krebsarten bei Frauen weltweit. 15-20% der Brustkrebspatientinnen leiden an dem HER2 / neu-positiven primären Brustkrebstyp ; diese aggressive Krebsform besitzt eine genetische Verstärkung, die zu einer Überexpression des HER2-Proteins führt. Trastuzumab wird als Erstlinientherapie eingesetzt, während Trastuzumab-Emtansin (T-DM1) eine Standardbehandlung ist, die als Zweitlinientherapie bei fortgeschrittenem HER2-positivem metastasiertem Brustkrebs verwendet wird. T-DM1 besteht aus dem monoklonalen Antikörper Trastuzumab, der mit einer zytotoxischen Substanz gekoppelt ist, das aus dem äthiopischen Strauch Maytenus serrata isoliert wurde. Die meisten Patienten entwickeln jedoch innerhalb eines Jahres eine Resistenz gegen T-DM1. Mehrere Resistenzmechanismen werden vermutet, aber nur wenige wurden bisher erforscht. In dieser Arbeit wurden zwei dieser möglichen Resistenzmechanismen genauer beschrieben : eine Veränderung der lysosomalen Funktion sowie eine abnorme CyclinB1 / Cdk1-Expression. Um eine Veränderung der lysosomalen Funktion zu bestätigen wurden pHrodo Farbstoffe verwendet und eine pH-Wert erhöhung in den Lysosomen in resistenten Zelllinien festgestellt. Die Erhöhung des lysosomalen pH-Werts unter alleiniger Verwendung von Chloroquin und der Kombination mit T-DM1 war jedoch bei Zytotoxizitätstests aufgrund der hohen Variabilität der Ergebnisse schwer zu interpretieren, was wahrscheinlich auf die inhärente Toxizität von Chloroquin selbst zurückzuführen ist. Zusätzlich zu dem Anstieg des lysosomalen pH-Werts mit der Resistenz gab es einen Anstieg der Lysosomen Anzahl pro Zelle mit zunehmender Resistenz gegen T-DM1. Die Cathepsin-Expression, das T-DM1-spaltende Enzym, hatte geringen Einfluss auf die Resistenzentwicklung. Ein weiterer Kandidat, der CyclinB1 / CdK1-Komplex, könnte ebenfalls für die Wirkung von T-DM1 entscheidend sein, da DM1 nur in der M-Phase der Zelle wirkt, in der die Spindelanordnung durch T-DM1 gestört wird. Unsere Hypothese, dass ein abnormer Komplex zur Zellresistenz führt, konnte jedoch durch verschiedene Experimente widerlegt werden. Im Gegenteil, die CyclinB1-Expression nimmt sogar mit zunehmendem Resistenzniveau zu, was auch mit den kürzeren Generationszeiten resistenter Zellen im Vergleich zu ihrer sensitiven Mutterzelllinie zusammenfällt. Interessanterweise hatte die T-DM1-Resistenz keinen Einfluss auf die DNA-Synthese, wie BrdU-Assays zeigten. T-DM1 führt allerdings zu einer Erhöhung von

CyclinB1 sowohl in den sensitiven als auch in den resistenten Subklonen. Zusammenfassend kann gesagt werden, dass eine fehlerhafte Expression von CyclinB1 keinen direkten Einfluss auf die T-DM1-Resistenz hat. Es kann jedoch festgestellt werden, dass die Antikörper-Wirkstoff-Konjugate zu einer Akkumulation von CyclinB1 in allen Zelllinien führt. Im Gegensatz dazu konnte ein veränderter lysosomaler pH-Wert als möglicher Resistenzmechanismus bestätigt und in resistenten Zelllinien auch eine erhöhte Anzahl von Lysosomen nachgewiesen werden.

Table of Contents

1 Introduction

1.1 Breast cancer: HER2/neu

There are three types of breast cancer: ER-positive, HER2-positive and triple negative. These distinctions are very important for the appropriate form of treatment. 80% of all breast cancers are ER-positive which means that the cells grow because of the hormone estrogen. In the HER2-positive breast cancer cells, the HER2 protein is overexpressed and the triple-negative breast cancer is tested negative for the hormones estrogen, progesterone and HER2, which is the most aggressive form (Ballinger, Kremer, and Miller 2016).

HER2 (human epidermal growth factor receptor 2) is a tyrosine kinase receptor located in the plasma membrane of the cells. This oncogene belongs to the ErbB (epidermal growth factor receptor) family which includes the following receptors: EGFR / HER1, HER2, HER3 and HER4. The HER receptors involve an extracellular domain, a transmembrane helix, a cytoplasmic kinase domain and a C-terminus. EGFR family ligands include EGF, TGFα, HB-EGF, epi- and Amphiregulin, betacellulin and various isoforms of the heregulin / neuregulin family. A special exception within the HER family are the HER2 and HER3 receptors because HER2 has no extracellular ligand binding domain and HER3 does not possess intrinsic kinase activity which can be observed in Figure 1 (Lapper et al. 1999). As a consequence, HER3 cannot form homodimers and a co-receptor from the HER family like HER2 is needed. Heterodimers are more stable than homodimers, which means that the signals are stronger, and the tumour is more aggressive. If the HER2 protein is overexpressed in cells, it is an indicator for poor prognosis in breast cancer tumours which is the case in 20% of mamma carcinomas (Mitri, Constantine, and Regan 2012). The formation of the HER2/HER3 heterodimer complex induces phosphorylation of tyrosine residues which further activate two signaling cascades. The signaling cascades which were activated are the PI3K / Akt and the Ras / Raf / MEK / MAPK pathways (Garrett and Arteaga 2011).

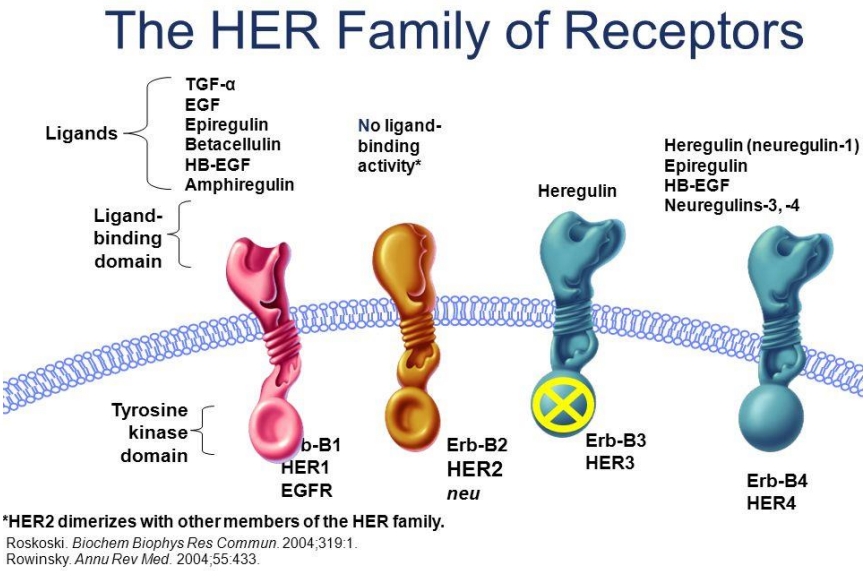

Figure 1 Overview of the HER receptors. The HER family contains the HER1, HER2, HER3 and HER4 receptors (Rowinsky.Annu Rev Med, 2004).

HER2 forms heterodimers also with other EGF receptors which can activate different signaling cascades. Which pathway is activated depends mainly on the composition of the HER2 dimer. The HER2 / HER3 and HER2 / HER4 heterodimer complexes which bind the ligand heregulin activate the PI3K-PKB / Akt pathway. In the HER3 the intrinsic kinase action is missing, but with its six docking sites the receptor is able to potently activate the phosphatidylinositol-3 kinase (PI3K)/Akt signaling pathway. The PI3K-Akt pathway has many downstream effects and promotes survival and growth. The pathway must be carefully regulated. There are many ways in which the signaling pathway can be negatively regulated, one possible reason would be the reduction of the PIP3 levels which leads to the loss of PTEN (Figure 2). Loss of PTEN, which works as a tumour suppressor, leads to over-activation of Akt which is the case in most cancer cells. The Akt kinase, which is a key effector of PI3K, is activated at the PI3K receptor complex and regulates cell proliferation and survival of tumour cells. HER2 and EGFR have sequence motifs in the C-terminus for the binding of adapter proteins such as Grb-2 or Shc, which induce recruitment of Ras. In contrast, phospholipase C can bind directly to the activated EGFR or HER2 receptor via an SH2 binding motif (Morgan et al. 2010). The activation of these signal cascades finally results in the activation of transcription factors in the nucleus, which

are the regulation genes for cell proliferation, cell adhesion or cell differentiation (Eccles 2002).

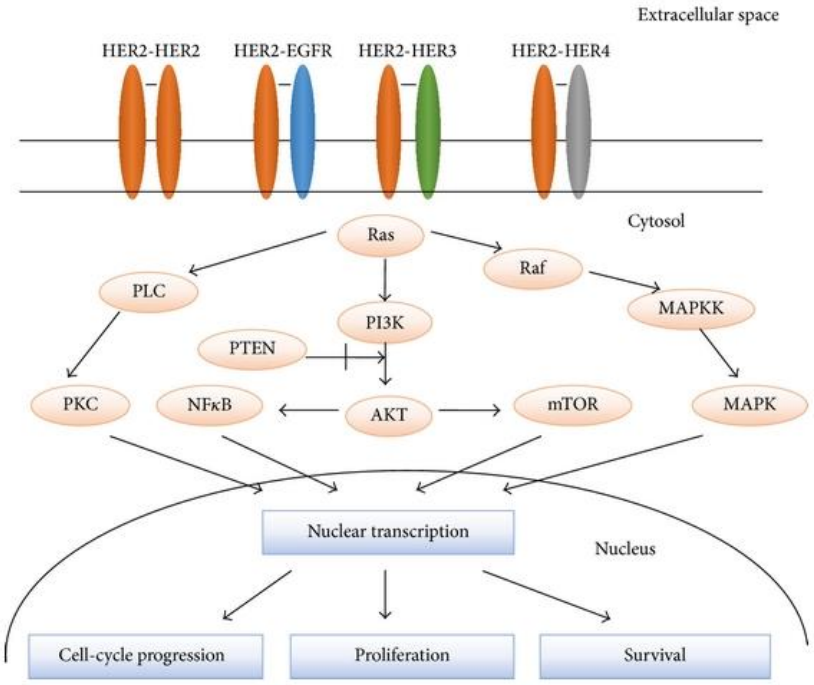

Figure 2 Her2 downstream signaling cascade (Iqbal and Iqbal 2014)

1.2 T-DM1: mechanism of action

T-DM1 is the abbreviation for Trastuzumab emtansine, which is a recombinant humanized monoclonal antibody linked to a cytotoxic agent. Mertansine, the cytotoxic agent, is a tubulin inhibitor, meaning that it inhibits the assembly of microtubules. It was originally isolated from the Ethiopian shrub Maytenus serrata. This antibody-drug conjugate is mainly used in the treatment of HER2 positive breast cancer and gastric cancer. TDM1 is obtained by the conjugation of trastuzumab connected by a stable thioether linker to the antimicrotubule agent maytansine (DM1) (Martínez et al. 2016) (Galanternik et al. 2016). The mechanism of trastuzumab at the molecular and cellular level is described in many studies in the past decades, so the binding to HER2 receptor prevents the activation of the signaling pathways like Ras / MAPK or PI3K / Akt. Furthermore, there is some evidence that trastuzumab also inhibits angiogenesis.

Treatment with trastuzumab leads to a decreased expression of VEGF (vascular endothelial growth factor), TGF-α (transforming growth factor-α), Ang-1 (angiopoietin-

1) and PAI-1 (plasminogen activator inhibitor-1), which usually have an impact on blood vessel formation and vascularization of the tumor (Wen et al. 2006).

The binding of T-DM1 with the Her2 receptor on the surface of the cell leads to uncoupling of ligand-independent HER2-HER3 heterodimers and inhibition of downstream signaling. Via receptor-mediated endocytosis, T-DM1 is transported into the cytosol and subsequently into lysosomes which is shown in Figure 3 below. In the lysosomes, the antibody-drug conjugate is cleaved by lysosomal proteolytic breakdown into its individual components. The cleavage process takes place mainly by cathepsin which can work optimally in acidic pH (Barok, Joensuu, and Isola 2014). In previous literature no detailed mechanism explained how DM1 is released from the lysosome into the cytosol, but it is expected that it takes place either through diffusion or via different transporters for example the lysosomal transporter SLC46A3 (Li et al. 2018). After cleavage of the toxin, the monoclonal antibody is either immediately degraded or transported to the surface of the cell for recycling. DM1, on the other hand, is transported to the cytosol where it can act on tubulin and inhibits the microtubule polymerization during mitosis, which leads to either mitotic arrest, mitotic catastrophe, disrupted intracellular trafficking or apoptosis. DM1 and its metabolites need to accumulate in the cytoplasm to reach a concentration that exceeds the threshold needed to cause apoptosis. Low tumor HER2 expression, poor internalization of the HER2-T-DM1 complexes, defective intracellular and endosomal degradation of T-DM1 are all related to a reduced intracellular DM1 level (Barok et al. 2011) (Martínez et al. 2016).

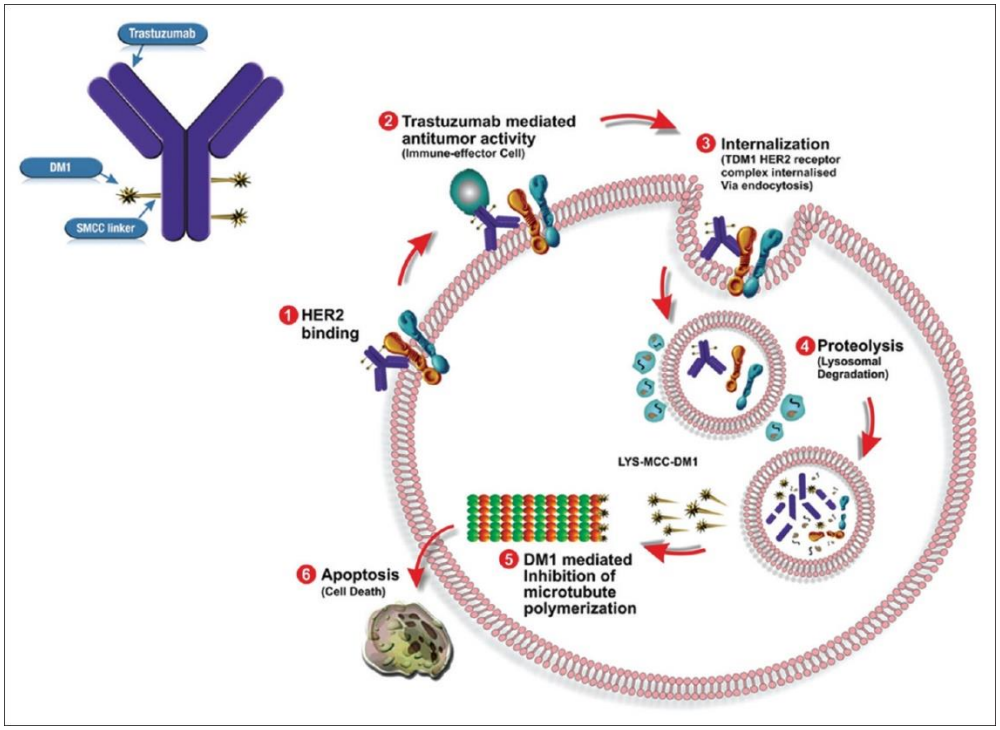

Figure 3 The mechanism of action of T-DM1 (Gogia and Nigade 2018)

1.3 T-DM1 resistance

70% of HER2 positive cancer patients develop resistance against T-DM1 after one year of treatment. In previous studies a down-regulation of HER2 was observed after T-DM1 resistance, but other HER2-target agents were still effective, suggesting that the reduction of HER2 had no direct effect on T-DM1 resistance (Galanternik et al. 2016). Among the several ways how T-DM1 resistance can develop, one option could be a weak uptake of T-DM1 or a defective intracellular transport. SLC46A3 or similar transporters, that are responsible for intracellular DM1 trafficking, could be downregulated which could prevent the binding of maytansinoid metabolite to tubulin (Gagliato et al. 2016). Also, the protein MUC4 and CD44 prevent the binding of trastuzumab in different ways. While CD44 causes an increased internalization of the HER2 receptor, the membrane-associated glycoprotein MUC4 masks the binding site of the receptor. Another resistance mechanism against HER2 inhibitors is a mutation of the target molecule itself, which can lead to alteration of drug binding. In previous studies, patients with metastatic breast carcinoma cytosolic expression of p95-HER2 show a very low response to trastuzumab treatment compared to patients without p95-HER2 in their tumors (Kocar et al. 2014). The upregulation of ligands which can lead to proliferation and cell death inhibition is also described as a resistance mechanism against trastuzumab emtansine. Neuregulin 1 is a ligand for HER3 and

HER4 receptors. It induces heterodimerization of HER3 with other EGFR receptors (mainly HER2), resulting in phosphorylation of tyrosin residues which further activate the PI3K signaling pathway and Ras/Raf/MAPK pathways. Expression of Neuregulin causes a higher proliferation than ErbB2 overexpression, so it can inhibit the cellular response to T-DM1 (Nonagase et al. 2016) (Peddi and Hurvitz 2014).
Molecular mechanisms of trastuzumab resistance may also involve a constitutive activation of the PI3K / Akt signaling cascade. The increased activity results either because of a reduced expression of the endogenous Akt inhibitor PTEN or by activating mutations in the catalytic subunit of PI3K which can be seen in Figure 4 (Gagliato et al. 2016) (Lavaud and Andre 2014). Also, a reduced expression of the CDK inhibitor p27kip1 or a JAB1-dependent, increased degradation of p27kip1 may contribute to resistance against Trastuzumab emtasine (Nahta, Hung, and Esteva 2004). A modified or mutated tubulin may lead to resistance because maytansine (DM1) can no longer bind to the altered tubulin structure. Mutations lead to an increase in the amount of polymerized tubulin which results in continuous proliferation. DM1 therefore leads to the inhibition of microtubulin polymerization by binding to specific binding sites on the surface of alpha and beta tubulin and thereby destabilizing microtubulin. Microtubulin play an essential role in cell cycle processes like mitosis and the activity of cell surface receptors (Sauveur et al. 2017) (Kavallaris 2010). Altered lysosomal function is also associated with T-DM1 resistance. For optimal enzyme functioning an acidic pH is essential, in resistant cells a higher pH (basic) is assumed, which would not lead to a complete proteolytic cleavage of the T-DM1 complex (Ríos-Luci et al. 2017). Another important resistance mechanism and pharmacodynamic predictor in HER2 positive breast cancer is the CdK1/cyclinB1 complex. The whole cell cycle is regulated by kinase activity and for the mitotic entry the cyclin dependent kinase 1 (CdK1) in complex with cyclinB1 is responsible. The activity of CDK1-cyclinB1 is regulated by the expression of cyclinB1. DM1 intervenes in the M phase of the cycle, so a cyclinB1 knockout would lead to a resistance (Sabbaghi et al. 2017a).

Most resistance mechanisms have been mainly studied for trastuzumab, but it is assumed that most of them also apply for the antibody-drug complex T-DM1. In this work, the resistance mechanisms suspected for T-DM1 were investigated. These would be an altered lysosomal function and an aberrant CdK1/cyclinB1 complex.

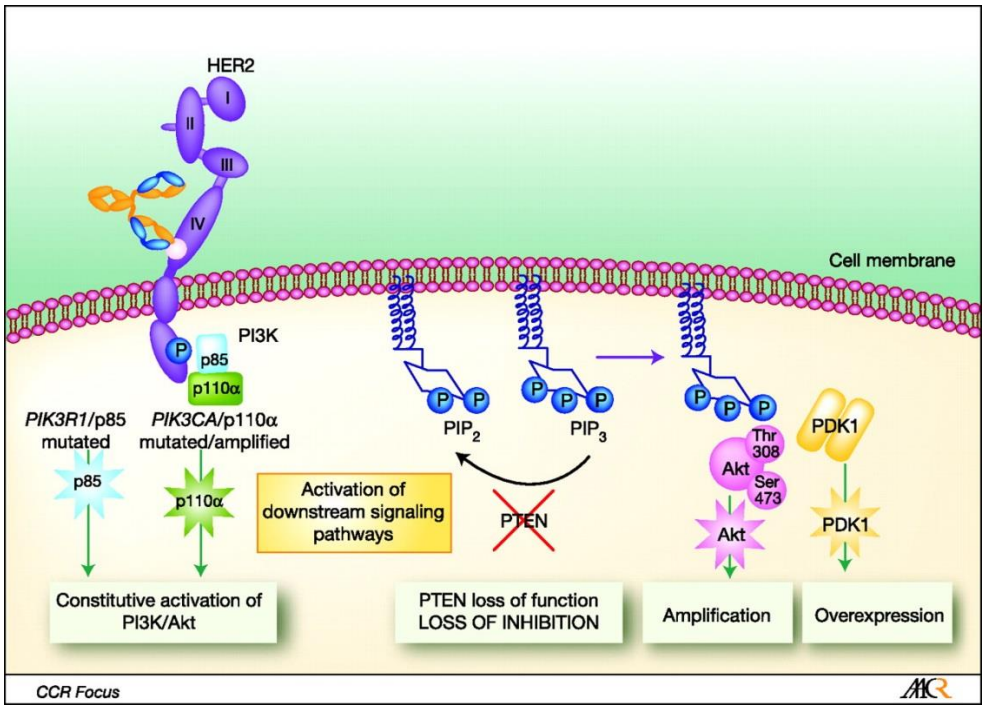

Figure 4 Resistance mechanism of Trastuzumab (Pohlmann, Mayer, and Mernaugh 2009)

1.3.1 Alteration in lysosomal functions

Lysosomes are cell organelles which have an essential part in the digestive system of a cell. Lysosomes are acidic vesicles which contain hydrolytic enzymes like cathepsin for macromolecule digestion. For optimal activity, these enzymes require a pH between 4-5 (Lu et al. 2017). The acidic pH in the lysosomes is a protective mechanism in case the lysosome is damaged, because in a neutral pH environment such as the cytosol, the enzymes are inactive. The low pH within the lysosomes is maintained via lysosomal membrane, surrounded by V-type ATPase transporters which pump protons against the electrochemical gradient into the lysosomes. The membrane proteins are highly glycosylated on the inside to protect against self-digestion (Fennelly and Amaravadi 2017).

The lysosomal function as reported previously is probably essential for the efficacy of T-DM1, so an altered function can be associated with a T-DM1 resistance. As already mentioned for the optimal function of the lysosomal proteolytic enzymes an acidic pH in the lysosome's lumen is crucial. In resistant cells, a neutral or slightly basic pH is assumed, resulting in reduced enzyme activity which prevents acceptable cleavage of T-DM1 (Ríos-Luci et al. 2017) (Piao and Amaravadi 2016). Lysosomes

also play an essential role in cell apoptosis and the hydrolytic enzymes can promote tumorigenesis; an overexpression of these proteases is often associated with a poor prognosis. Therefore, lysosomes and lysosomal enzymes are good target molecules for cancer therapy. Furthermore, lysosomes can also bind cancer medication through their acidic milieu, thus weakening their effect, which is why lysosomes are also a focus of attention in resistance mechanisms (Piao and Amaravadi 2016). One of the most studied lysosomal proteases is cathepsin. Cathepsins are small proteins that have optimal activity at acidic pH. Cathepsin also plays an essential part in tumorigenesis: depending on the location of the cathepsin, it can suppress or promote tumor growth. Furthermore, an association between overexpression of cathepsin and tumor aggressiveness was found, as releasing proteases can promote cell detachment and thus facilitate metastatic effects. Cathepsin also shows a sensitization of chemotherapeutic agents and an inhibition of the enzyme could increase the effect of drugs (Fennelly and Amaravadi 2017) (Fehrenbacher et al. 2005).

An effective lysosome function has a huge impact on cancer cells. In metastatic cells or in aggressive cancer cells, significant changes in the lysosomal structure and function can be detected. An altered lysosome volume, distribution of the lysosomes as well as an altered enzyme activity can be observed in those cells. Due to the accumulation of lactic acid, cancer cells have a more acidic extracellular milieu than normal cells. Energy production in normal cells is mainly ensured by mitochondrial oxidative phosphorylation, while in tumor cells it is produced by glycolysis followed by lactic acid fermentation (Kato et al. 2013). As already confirmed in literature, the extracellular acidic environment of cancer cells has an effect on the size, number and arrangement of lysosomes in the cell. In high-metastatic breast cancer cells, mostly larger but fewer lysosomes were observed. In addition, most lysosomal compartments in cancer cells were closer to the cell periphery than in the perinuclear area (Glunde et al. 2003).

1.3.2 Aberrant Cdk1/Cyclin B1 complex

A eukaryotic cell runs through four phases in the cell cycle called G1, S, G2 and M phase. The Gap phase 1 (G1) also known as the first grow phase, prepares the cells for DNA synthesis, the following phase is the synthesis phase (S-phase) where DNA replication takes place. In the Gap phase 2 (G2) cells grow continuously and they prepare for mitosis. The last phase is the mitosis (M-phase), where chromosomes are separated, and cell division occurs. Regulation of the cell cycle includes processes essential for cell survival, such as growth, repair and damage of the cell. The two main cell cycle regulatory molecules are cyclin and cyclin-dependent kinases. Different cyclin/Cdk complexes are involved in different cell cycle transitions (Figure 5). Cyclin-dependent kinases (Cdk) need to form a complex with cyclin for activation. The activity of CDK-cyclin is regulated mainly by the expression of cyclin. The most important complex in T-DM1 resistance is the cdk1/cyclin B1 complex which is responsible for the progression from G2 into M-phase of the cell.

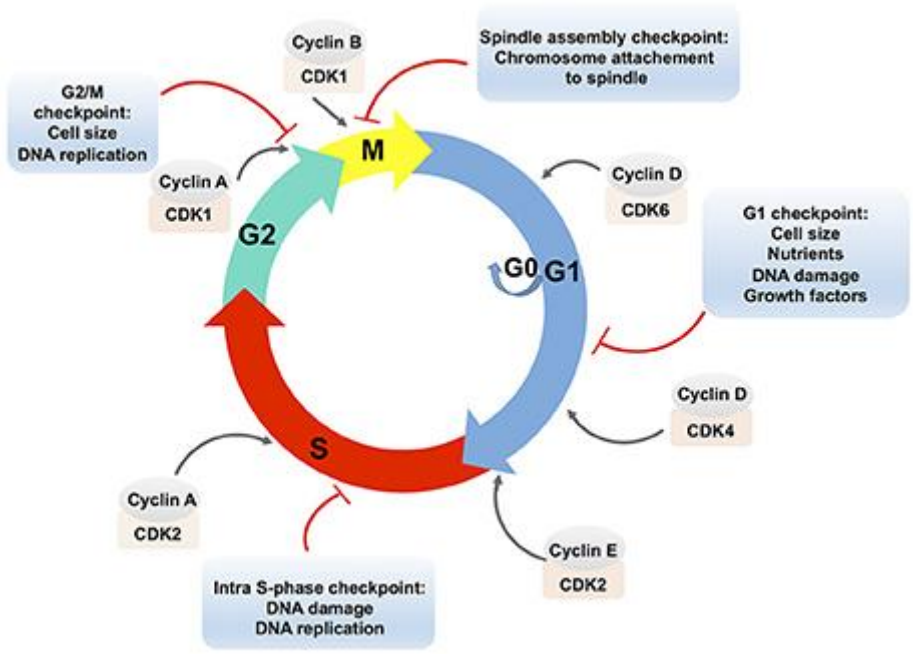

Figure 5 Representation of the eukaryotic cell cycle and its regulation. The eukaryotic cell cycle consists of the G1 and the G2 phase, the S-phase, and the M (mitosis) phase. Cells can also enter a quiescent state, the G0 phase. The cell cycle is regulated by cyclin / cyclin-dependent protein kinase (CDKs) complexes (Filho, Nicolas, and Castro 2017).

Cyclin levels oscillate over the course of the cell cycle; cyclin B1 increases in the G2 phase so that the cyclinB1-cdk1 complex can accumulate. The complex is usually

inactive in the G2 phase and becomes active only in the M phase, where it leads to significant changes in microtubule dynamics. The cyclinB1/ cdk1 complex is a key enzyme for mitosis and is involved in the collapse of the nuclear envelope and the spindle pole assembly (Lindqvist et al. 2007). CyclinB1 is located in the cytoplasm before the M phase and is transported after phosphorylation into the nucleus. The phosphorylation also avoids the transfer from the nucleus by blocking the nuclear export signal (Aaltonen et al. 2009). As is already known, cyclinB1 is responsible for the transport of the cell from the G2 phase to the M phase, but in cancer cells it may be the case that cyclinB1 is over-expressed, leading to uncontrolled cell growth. Overexpression of the enzyme leads to an increased binding of cdk1, which in turn induces phosphorylation of other substrates, which can lead to a higher rate of unregulated proliferation. The cyclin B1 concentration in cells may also be associated with a poor prognosis. The cyclin B1 level could be a predictor of tumor invasion and a higher probability of metastasis. In mamma carcinoma cells it was already shown that the cyclin B1 concentration was significantly increased and favored the formation of lymph node metastasis (Choi, Fukui, and Zhu 2011). Further studies also showed that trastuzumab emtasine leads to accumulation of cyclin B1 in sensitive cells, but this phenomenon could not be observed in resistant cells. In this paper, it was also possible to detect a resistance development of sensitive mother cell lines by breaking down cyclinB1 via siRNA (Sabbaghi et al. 2017b). In HER2-positive breast cancer explants, absence of cyclin B1 correlated with T-DM1 failure to induce apoptosis (Song et al. 2008). In sensitive mother cell lines, the antibody-drug conjugate induced G2–M arrest and mitotic catastrophe. Mitotic catastrophe is a mechanism that senses mitotic failure and responds by driving a cell to an antiproliferative state of death or senescence. This phenomenon does not occur in resistant cells where it is assumed that the machinery for cell-cycle arrest is disrupted. Based on these results, we hypothesized a potential involvement of the cyclinB1 / cdk1 complex in T-DM1 resistance (Sabbaghi et al. 2017b).

1.4 Aim of the study

Breast cancer is an important disease worldwide. Many women are affected and therefore more and more treatments and therapies are being developed. But many patients develop resistance after a period of time against each therapy, so resistances and their causes play an important role nowadays. Unfortunately, many resistance mechanisms and how they develop are not fully investigated. The aim of this study was to shed further light on the resistance mechanism of trastuzumab emtasine in breast cancer cells, focussing on an alteration in lysosomal function and an aberrant in cyclin B1/Cdk1 complex.
Further, the aim of this study is to understand and describe T-DM1 resistance mechanism in order to improve the characterization of patients in diagnostics to make a better choice in the treatment of patients and to find the most effective therapy for each individual.

Based on this background knowledge, the following hypotheses were studied:

1) Do resistant cell lines have an altered lysosomal function and is it possible to turn sensitive cells into resistant ones by changing the pH of the lysosomes?

2) Is there a connection between the pH value in the lysosomes and the expression of cathepsin?

3) Does the cyclin B1/Cdk1 complex have an impact in T-DM1 resistance and is there a connection between cyclin B1 expression and the cellular generation time?

4) Do cyclin B1 and Cdk1 expression behave the same way in sensitive and resistant cells?

2 Materials and Methods

2.1 Cell Culture

The altered lysosomal function as well as the cyclin B1 expression was investigated in various mamma carcinoma cell lines, including the Her2/neu overexpressed SKBR-3 cell line which was derived from a pleural effusion due to an adenocarcinoma, which showed a very high response to T-DM1 treatment. The MCF-7 cell line which was used as negative control also originates from pleural effusion, in this cell line estrogen and progesterone receptors are present but no HER2 receptor. The MDA-468 cell line which also rarely responds to T-DM1 has no HER2/neu receptor on the surface as well, while T38 cells which are grown from the cell line MDA-468 and transfected with HER2/neu receptor show good response to T-DM1 treatment. All the T-DM1 resistant cell lines were established from the naive cell lines by continuous exposure to T-DM1 in different concentrations. The cell lines used for the following experiments are listed in Table 1.

Table 1 Characteristics of breast cancer cells used in the experiment

Cell line		T-DM1-resistance
SKBR-3	Naturally overexpressing Her2/neu; treatment with T-DM1 is effective	0 µg/ml
T38	Cell line MDA-468 transfected with Her2/neu	0 µg/ml
MDA-468	High number of epidermal growth factor receptor; rarely responding to T-DM1	0 µg/ml
MCF-7	estrogen and progesteron receptor positive; rarely responding to T-DM1	0 µg/ml
SKBR-3 + 0,003 µg/ml T-DM1	low resistant breast cancer cell line	0,003 µg/ml
SKBR-3 + 0,03 µg/ml T-DM1	intermediate resistant breast cancer cell line	0,03 µg/ml
SKBR-3 + 0,3 µg/ml T-DM1	high resistant breast cancer cell line	0,3 µg/ml
T38 + 0,01 µg/ml T-DM1	low resistant metastatic adenocarcinoma	0,01 µg/ml
T38 + 0,1 µg/ml T-DM1	intermediate resistant metastatic adenocarcinoma	0,1 µg/ml
T38 + 0,5 µg/ml T-DM1	intermediate resistant	0,5 µg/ml

	metastatic adenocarcinoma	
T38 + 1 µg/ml T-DM1	high resistant metastatic adenocarcinoma	1 µg/ml
MDA-468 + 0,5 µg/ml T-DM1	low resistant metastatic adenocarcinoma	0,5 µg/ml
MDA-468 + 1 µg/ml T-DM1	intermediate resistant metastatic adenocarcinoma	1 µg/ml
MDA-468 + 1,5 µg/ml T-DM1	high resistant metastatic adenocarcinoma	1,5 µg/ml

2.1.1 Cultivation of breast cancer cells

Materials

- T75 flasks (Corning®, Sigma-Aldrich)
- RPMI Medium 1640 (1x) + GlutaMAX™ (GIBCO®, Thermo Fisher Scientific)
- Fetal Bovine Serum (Sigma-Aldrich)
- Streptomycin/Penicilin (Lonza, 17602E)
- Accutase® solution for cell culture (Sigma-Aldrich)
- DPBS (1x) (GIBCO®, Thermo Fisher Scientific)

Procedure

Cells were cultivated in T75 flasks with RPMI 1640 medium containing GlutaMAX™ and 10% fetal bovine serum (FBS). T-DM1 resistant cells were additionally cultured with adequate T-DM1 concentrations, which were diluted in RPMI medium. Cells were cultivated to a confluence of 80% and split twice a week. All work was carried out under laminar flow. For splitting the cells, the medium was removed first and cells were washed with DPBS afterwards. 2 ml accutase was used to detach the cells from the surface by incubation at 37°C for 5 minutes. Afterwards, the reaction was neutralized with RPMI 1640 + GlutaMAX™ + 10% FBS medium. After centrifugation at 287g for 5 minutes, the resulting pellet was resuspended again in RPMI medium and then an adequate amount of cell suspension was transferred back into the flasks and incubated again at 37°C and 5% CO_2.

2.2 Cell Culture assays

2.2.1 MTT assay

The MTT assay is one of the simplest assays using 3-[4,5-dimethylthiazol-2-yl]-2,5-diphenyl tetrazolium bromide (MTT). The MTT assay assesses the viability of cells in the cell culture by allowing the water-soluble yellow dye (MTT) to be taken up in viable cells and reduced by the action of mitochondrial dehydrogenases. The reduction product of the colorimetric assay is a water-insoluble blue formazan (Horton et al. 2011).

Half maximal effective concentration (EC_{50}) of an antibody-drug conjugate like Trastuzumab emtansine (T-DM1) can be determined with the MTT assay by measuring the absorbance at 570 nm of cells exposed to a logarithmic dilution series. As the cytostatic concentration increases, the colour changes to yellow, meaning that the cells are dead.

MTT assays were performed with sensitive and resistant cell lines incubated with different T-DM1 concentrations and chloroquine concentrations, which should increase the pH in the lysosomes of the cells.

Materials

- 6mg/ml Trastuzumab emtansine (T-DM1)
- Chloroquine (Invivogen)
- DPBS (1x) (GIBCO®, Thermo Fisher Scientific)
- 98% MTT (Sigma-Aldrich) salt solution in DPBS (GIBCO®, Thermo Fisher Scientific)
- Solubilization solution (40% N,N-Dimethylformamid, 20% SDS; adjusted to pH-value of 4.5 - 5 with CH_3COOH)
- RPMI Medium 1640 + GlutaMAX™ (GIBCO®, Thermo Fisher Scientific)
- Fetal Bovine Serum (Sigma-Aldrich)
- Streptomycin/Penicilin (Lonza, 17602E)
- 96 well plates

Procedure

Cells were harvested and then sown in triplets in 96 well plates (10000 cells/well in 100µl). To count the cells. a Bürker-Türk chamber was used. Cells were incubated with medium for 24 h at 37°C under 5% CO2 and then 25 µl of the corresponding T-DM1 or chloroquine concentration added to the cells and substituted with medium to a final volume of 150 µl. The plate was wrapped in aluminum foil and incubated at 37°C for 72 h (3 d). After 72 h, the dye solution (15 µl /well) was added to each well and incubated again for 4h at 37°C. Before the plate could be analysed, 100 µl stop solution were added and the plate was incubated for another 24 h at room temperature. The absorbance was measured with the Biochrom Asys Expert Plus Microplate Reader: extinction 570 nm, reference wavelength 690 nm. The data was analysed with the software GraphPadPrism 4.0 using a nonlinear regression for curve fitting resulting in a sigmoidal dose-response curve.

2.2.2 PDT assay

The cell population doubling time is the time it takes cells to complete one cell cycle and double. This analysis is carried out by MTT assay. In this way, it can also determine the influence of substances on the ability to divide or the vitality of cells. An exponential growth arises at a constant relative growth rate from which a constant doubling period can then be calculated.

Materials

- DPBS (1x) (GIBCO®, Thermo Fisher Scientific)
- 98% MTT (Sigma-Aldrich) salt solution in DPBS (GIBCO®, Thermo Fisher Scientific)
- Solubilization solution (40% N,N-Dimethylformamid, 20% SDS; adjusted to pH-value of 4.5-5 with CH3COOH)
- RPMI Medium 1640 + GlutaMAX ™ (GIBCO®, Thermo Fisher Scientific)
- Fetal Bovine Serum (Sigma-Aldrich)
- Streptomycin/Penicilin (Lonza, 17602E)
- 96 well plates

Procedure

The procedure is similar to the MTT assay, the cells are grown in triplets (3000 cells and 5000 cells) and according to the time points on 4 different 96 well plates. The cells were counted exactly via Bürker-Türk chamber and then pipetted into each well in 150 µl. At four consecutive time points (24 h, 72 h, 120 h, 144 h) 15 µL MTT salt solution were added to each well. After the incubation time (4 h) at 37° C, 100 µL of solubilization solution were added and another incubation period of 24 hours at room temperature followed. The photometric evaluation was carried out by Biochrom Asys Expert Plus Microplate Reader at 570 nm. The software GraphPadPrism 4.0 was used to analyze the data by plotting the extinction against the time periods. The slope of the resulting curve (m) was used to calculate the population doubling time according to Equation 1.

$$PDT = \frac{log2}{m} \qquad \text{Equation 1}$$

2.3 BrdU incorporation assay

5-bromo-2'-deoxyuridine (BrdU) is an counterpart of the nucleoside thymidine used in the BrdU assay to identify proliferating cells. BrdU is incorporated into DNA of living cells. A BrdU specific monoclonal antibody was used to label the cells during the S phase of the cell cycle, which can show in which cell line most of the cells are in the synthesis phase.

Materials

- BrdU cell proliferation assay kit (Cell Signaling Technology)
- RPMI Medium 1640 + GlutaMAX™ (GIBCO®, Thermo Fisher Scientific)
- Fetal Bovine Serum (Sigma-Aldrich)
- Streptomycin/Penicilin (Lonza, 17602E)
- 96 well plates

Procedure

Cells were grown in triplets in 96 well plates (10000 cells /100µl per well) and incubated at 37°C for 48h. After incubation, the prepared 10x BrdU solution was added to the cells to reach a final concentration of 1x BrdU in the wells. Subsequently, a further incubation period of 24 h was necessary and then the medium was removed after a centrifugation step (300 g for 10 min). 100µl/well of the

fixing /denaturing solution were added and left to incubate at room temperature for 30 minutes. Afterwards the solution was removed and 100 µl/well of the prepared 1x detection antibody solution was added and incubated 1 hour at room temperature. After incubation step the solution was removed as well and 3 washing steps were followed (1x wash buffer). Additionally, 100µl / well of the 1x HRP conjugated secondary antibody solution were added and incubated at room temperature for 30 minutes. Subsequently the solution was removed, and the cells were washed 3 times with 1x washing buffer and then 100µl TMB substrates was added. Another incubation step for 30 minutes takes place before 100µl stop solution was added and the cells were measured at 450nm absorption.

2.4 Cathepsin D assay

Cathepsins are proteases found mainly in the lysosomes that become activated at lower (acidic) pH. There are many forms of cathepsins and some of them have important roles in mammalian cellular turnover. An increasing expression of cathepsin can be related to the aggressiveness of the tumor and poor prognosis. There is also evidence that invasiveness of tumors shows a relationship to their content of lysosomal enzymes. Cathepsin shows also a sensitization of lysosome-targeting drugs and an inhibition of cathepsin can enhance chemotherapeutic response (Fennelly and Amaravadi 2017).

Materials

- Cathepsin D Activity Fluorometric Assay kit (BioVision)
- RPMI Medium 1640 + GlutaMAX^{TM} (GIBCO®, Thermo Fisher Scientific)
- Fetal Bovine Serum (Sigma-Aldrich)
- Streptomycin/Penicilin (Lonza, 17602E)
- Perkin Elmer Microplate (black)
- Thermo Fisher Scientific: Nunc A/S (white)

Procedure

Cells are counted after trypsinization, collected in a tube ($1x10^6$ cells) and centrifuged at 1200xg for 5 min. After medium removal, the pellet was lysed with 200 µl lysis buffer and placed on ice for 10 minutes. Next, the cells were centrifuged at top speed (3600xg, 5 min) and the clear cell lysates were transferred into new labeled tubes. Afterwards 25 µl of lysate (or 1-10ng of purified cathepsin D protein samples) were transferred to each well of a 96 well plate and fill up to 50µl with CD cell lysis buffer. Before incubating the plate for 2 h at 37 ° C, a master mix consisting of 50 µl reaction buffer and 2 µl substrate for each well was prepared and added to each well. After 2 hours the plate was measured via fluorometer with 328nm excitation filter and 460nm emission filter. The following settings were used to measure the cathepsin levels via spectramax: fluorescence intensity (FL), well scan read type (5; 1.125), shake off, and then either bottom measurement or top and integral time at 400ms or 40ms.

2.5 SDS-Page

Sodium-dodecyl-sulfate-polyacrylamide gel electrophoresis (SDS-PAGE) is a common separation method. This technique is used to separate proteins by their charge or molecular weight in an electrical field. The polyacrylamide gel matrix consists of an upper and a lower gel, the acrylamide/bis stacking gel has a porous structure, which is used to define a sharp band, while the lower acrylamide/bis separating gel has a defined and denser pore size, which is used for the separation of the proteins according to their size. Therefore, larger molecules migrate slower through the matrix than smaller ones. The proteins become visible through staining. The bands can be analyzed through the molecular mass to determine which band represents which protein (Roy and Kumar 2014).

Materials

- Solutions listed in Table 2
- Composition of gels shown in Table 3
- Precision Plus Protein Dual Color Standard (Bio-Rad)

Table 2 Solutions used for SDS-Page

Solution	Preparation
5x Tris-glycine buffer	125 mM Tris-Base (Merck) 1250 mM Glycine (Merck)

	0,5 % SDS (Pharmacia) dissolved in 1 L ddH2O, pH=8,3 (adjusted with HCl), filtered and stored at room temperature
2x Sample buffer	72 mM DTT (Dithiothreitol) (Merck) dissolved in 5 mL ddH2O, 5 mL 100 % glycerine (Merck), a tip bromphenol blue (Merck), 200µl aliquotes were stored at -20°C
1 M Tris-HCl	1 M Tris-Base (Merck) dissolved in 100 mL ddH20, pH=9,1 (adjusted with HCl), stored at room temperature
0,5 M Tris-HCl	0,5 M Tris-Base (Merck) dissolved in 100 mL ddH2O, pH= 6,8 (adjusted with HCl), stored at room temperature
10% SDS	Sodiumdodecylsulfate (Pharmacia) dissolved in 100 mL ddH2O, filtered and stored at room temperature
40% APS	Ammonium peroxydisulfate (Fluka) Dissolved in 1 mL ddH2O, stored in aliquotes at -20°C
Temed	BioRad

Table 3 gel composition for gel electrophoresis

Separation gel (10%)		Stacking gel (4%)	
Acrylamid/Bis 30%	1,5 ml	Acrylamid/Bis 30%	0,325 ml
ddH2O	1,5 ml	ddH2O	0,625 ml
1M Tris-HCl (pH=9.1)	1,9 ml	0.5 M Tris-HCl (pH=6.8)	1,55 ml
10% SDS	50 µl	10% SDS	25 µl
40% APS	10 µl	40% APS	4 µl
Temed	2,5 µl	Temed	2,5 µl

Procedure

For the SDS- Page, 10µg protein are needed. The sample was substituted to 10 µl with 1x Tris-glycine buffer and filled with 10 µl 2x sample buffer to a final volume of 20µl and denatured at 99,99 °C for 3 minutes. Afterwards, the probes were put on ice and centrifuged. 5 µl markers and the entire volume of samples (20 µl) were loaded onto the gel. 1x Tris-glycine buffer was used as electrophoresis buffer and the device was set up to 150 V for 60 minutes.

2.6 Western Blot

Western Blotting is a rapid immunoblotting technique for identifying specific proteins in a complex mixture of cell lysate. The protein mixture is separated into individual protein bands by SDS-Page and afterwards the protein of interest can be identified via chemiluminescence. Therefore, the electrophoresis membrane is first incubated with the primary antibody and then with the secondary antibody, which binds specific to the target protein. Chemiluminescent detection depends on incubation of the western blot with luminol/enhancer solution and stable peroxide solution. A signal can be detected corresponding to the position of the proteins (Jensen 2012).

Materials

- Solutions for Western blot listed in Table 4
- Whatman® paper (Thermo Scientific)
- PVDF membrane (0.45 µM, Thermo Scientific)
- Hyperfilm^{TM} ECL (GE Healthcare)

Table 4 Solutions for western blot analysis

Solutions	Preparations
Transfer buffer	39 mM glycine, 48 mM Tris-base 0,037% SDS (Pharmacia) and 20% methanol (Merck) dissolved and filled up with ddH_2O to 1l, filtered and stored by 4°C
10x Tris buffered Saline (TBS)	136.9 mM NaCl (Merck) 5.4 mM KCL (Merck) and 49.5 mM Tris-base (Merck) Dissolved in 1L ddH_2O, pH 7.4 (adjusted with HCL), after filtration stored at RT, 1x TBS was used for gel electrophoresis
SuperBlock Blocking Buffer in TBS	Thermo Scintific
Tween 20	0.5 M Tris base (Merck) Dissolved in 100 mL ddH_2O, pH 6.8 (adjusted with HCL), stored at RT
Super Signal West Dura Extended	Thermo Scientific

Procedure

For the semi-dry membrane transfer the required PVDF membranes and the 3MM Whatman paper need to be cut (9.5 x 7.5 cm). The transfer set up was as follows: positive electrode – Whatman® paper (conditioned in transfer buffer) – PVDF transfer membrane (conditioned first in methanol then in transfer buffer) – gel– Whatman® paper (conditioned in transfer buffer) – negative electrode for 1 h at 0.8 mA/cm2 membrane. Afterwards the transferred membrane was blocked for 2 h on the shaker in 15ml blocking buffer containing 0.05% Tween 20.
The blocked membrane was then incubated overnight at 4°C with 15 ml of a primary antibody (listed in table 5) solution which was diluted in blocking buffer + 0.05% Tween 20. The membrane was washed 5 times for 10 minutes with 20 ml 1xTBS (pH = 7.4) + 0.05% Tween 20. The membrane was then incubated 1h at the shaker with the secondary antibody (listed in table 6) solution which was also diluted with blocking buffer + 0.05% Tween 20. After another washing step the membrane was covered with a Luminol / Enhancer Solution and Stable Peroxide Solution which were mixed in a 1: 1 ratio, for 5 minutes at room temperature. Subsequently the membrane was dabed between Whatman papers and put into the transparent plastic foil without any air bubbles. Afterwards the blot was inserted into the film cassette, the required exposure time must be tested start at 1 minute and extend if necessary.

Table 5 primary antibodies used for Western Blot

primary antibody	dilution	secondary antibody	molecular weight	company	serial number
cyclinB1	1:1000	anti-rabbit	55kDa	santa cruz	Sc-752
Cdc2	1:200	anti-mouse	34kDa	santa cruz	sc-54
FoxM1	1:1000	anti-mouse	104-122kDa	santa cruz	sc-376471
GAPDH	1:5000	anti-rabbit	37kDa	santa cruz	FL-335

Table 6 secondary antibodies used for Western Blot

secondary antibody	dilution	primary antibody	company
Goat anti-mouse IgG (peroxidase conjugated)	1:100000	Cdc2	Thermo Scientific
	1:20000	FoxM1	
Goat anti-rabbit IgG (peroxidase conjugated)	1:50000	cyclinB1	Thermo Scientific
	1:200000	GAPDH	

2.6 PCR analysis

The expression of miRNA levels of breast cancer cells was identified via isolation of RNA followed by cDNA synthesis and real time PCR.

2.6.1 RNA isolation

The isolation of RNA is an essential method used in gene expression analysis. RNA isolation is often the most critical step, because of the presence of ribonuclease enzymes in cells which can degrade RNA. The RNA extraction can be divided into 5 steps: homogenization, phase separation, RNA precipitation, RNA washing and RNA solubilization.

Materials

- TRI Reagent® (Sigma Aldrich)
- Chloroform (Sigma Aldrich)
- Isopropanol (Sigma Aldrich)
- Ethanol 75% (Sigma Aldrich)
- 3 M Na-Acetate (pH=5.5)
- H_2O DEPC

Procedure

To lyse the mamma carcinoma cells without destroying their nucleic acids, TRI reagent was used. TRI reagent is a solution based on phenol and guanidine thiocyanate in a monophase solution that inhibits RNase activity. The cells were grown at 37°C and 5% CO_2 in T75 flask until 80% confluency was reached. The adherent cell monolayer was washed twice with DPBS before incubation with TRI reagent (1 mL) for 5 minutes. The cells were harvested via cell scraper; while 1 mL were used for further RNA isolation, the rest was stored at -80°C. To separate the solution in an aqueous phase (RNA), interphase (DNA) and an organic phase (protein) 0.2 mL chloroform was added to the cell lysate. Before the separation process via centrifugation (12000 x g for 15 minutes at 4°C) occurred, the cell lysate was vortexed (15 seconds) and incubated at room temperature (15 minutes). From this step on the samples were always kept on ice. The upper RNA phase was then

transferred to a new tube containing the same volume of chloroform. Before centrifuging the samples again (at 12000 g for 15 minutes at 4°C), the tubes were incubated 5 minutes at room temperature. For the RNA precipitation the upper phase was transferred into a new tube and 0.5 mL isopropanol were added and mixed with the pipette followed by 10 minutes incubation at room temperature. After that, another centrifugation step (12000xg for 15 minutes at 4°C) took place. To wash away any salt residue from the RNA pellet 1 mL ethanol (75%) was used. The washing process had to be very slowly and carefully, first the pellets were dried on air before being dried at 37°C for 10 minutes. Dissolve the clean RNA in 30-70 µl of DEPC H2O (depending on the size of the pellet) to ensure stability for long term storage. The RNA quality control can be accessed via Nano Drop® 1000 Spectrophotometer (Thermo Fisher Scientific). The concentration of the RNA samples was determined at 260 nm and H_2ODEPC was used as blank. The ratio of the absorbance at 260 nm and 280 nm was used to access the RNA purity. Values between 1.8 and 2 indicate pure RNA. The concentration of isolated RNA was calculated as shown in Equation 2.

$$\boldsymbol{RNA}\ [\tfrac{\mu g}{mL}] = \boldsymbol{OD600} * \boldsymbol{40}\ \tfrac{\mu g}{mL} * \boldsymbol{dilution\ factor} \qquad \text{Equation 2}$$

2.6.2 cDNA-Synthesis

The cDNA is a DNA which is synthesized by the enzyme reverse transcriptase from RNA (such as mRNA and ncRNA). The complementary DNA This is equivalent to the template strand of the duplex DNA. The cDNA copies of mRNA contain primarily sequences that encode protein. Therefore, cDNA clones are useful for many studies of gene function.

Materials

- 5x miScript HiFlex (Qiagen)
- 10x miScript Nucleics Mix (Qiagen)
- RNase free water (Qiagen)
- miScript Reverse Transcriptase Mix (Qiagen)

Procedure

The isolated RNA was transcribed into cDNA with the miScript II RT Kit (Qiagen; Cat. No. 21816). The RNA of all samples was diluted to a concentration of 10 ng in 5 µL RNase free water (= 2 ng/µL). The Master Mix was prepared as shown in table 5 below. For the negative cDNA control 10 µl Master Mix + RNase free water was used. The cDNA synthesis was then performed with the thermocycler PX2 for 60 minutes at 37°C and 5 minutes at 95°C. Afterwards the cDNA was either used for qPCR or stored at -20°C.

Table 7 reagents for cDNA-synthesis

Reagents	Conc.	µl/reaction
miScript HiFlex buffer	5x	3
miScript Nucleics mix	10x	1.5
RNase free water	/	4
miScript Reverse Transcriptase Mix	/	1.5
total volume		10 µl MM+ 5 µl RNA-probe (2 ng/µl)

2.6.3 Quantitative Real Time PCR

Real time-PCR, is a kind of the polymerase chain reaction that typically measures microRNA expression levels. Quantitative real time PCR needs cDNA probes, a specific forward primer, a universal reverse primer enzyme and SYBR green fluorescence for detection. RT-qPCR is used in some applications including gene expression analysis, RNA validation, microarray validation, pathogen detection, genetic testing, and disease research (Decallonne and Bouillon 2003).

Materials

- QuantiTect SYBR Green PCR Master Mix (Qiagen)
- miScript Universal Primer (Qiagen)
- miScript Primer Assay for the different miRNAs (Qiagen)
- RNase free water (Qiagen)

Procedure

For the RT-qPCR the miScript SYBR Green PCR Kit from Qiagen was used. The cDNA probes were diluted 1:10 with RNase free water before they were used for qPCR. The RT-qPCR was prepared as shown in table 8 below according to the Qiagen protocol. The Polymerase chain reaction was performed in a 72-well rotor of the RotorGeneQ and the qPCR program was set as follow: 1. Hold for 15 minutes at 95 ° C, 2. Cycling: denaturation 15 sec, 94 ° C; annealing for 30 sec, 55 ° C and extension 30 sec, 70 ° C, total cycle number of 40.

The qPCR data was then analyzed on the basis of “delta Cp” (ΔCp) or “delta delta Ct” (ΔΔCt) values. The CP value can be measured via several algorithms. The real efficiency was used for calculations. RNU48 which is constantly expressed in all cells is used as reference in all samples. The microRNA expression levels were calculated against the reference using the mathematical model for relative quantification in real-time qPCR according to (Pfaffl 2004).

$$Ratio = \frac{(\mathrm{Etarget})^{\Delta \mathrm{Ct}\,\mathrm{target}(\mathrm{control-sample})}}{(\mathrm{Eref})^{\Delta \mathrm{Ct}\,\mathrm{ref}(\mathrm{control-sample})}}$$ Equation 3

Table 8 reagents for RT-qPCR

Reagents	Conc.	µl/Ansatz
QuantiTect SYBR Green PCR Master Mix	2x	5
miScript Universal Primer	10x	1
miScript Primer Assay	10x	1
RNase-free water	/	1.67
Volume		8.67 µl MM +1.33 µl cDNA (1:100)

Table 9 QuantiTect primer assay

Primer	company	serial number
Hs_CCNB1_1_SG	qiagen	QT00006615
Hs_CDK1_1_SG	qiagen	QT00042672
Hs_CDK2_1_SG	qiagen	QT00005586

2.7 Fluorescence staining

2.7.1 Intracellular pH detection (pHrodo)

Intracellular pH is closely regulated by many cellular functions and has an impact on ionic homeostasis, apoptosis or cell cycle. The normal physiological pH is around 7 and 7.4, but it can vary between different organelles. In lysosomes normally a pH of about 4.5-5.5 is measured. Extracellular pH is typically higher than intracellular pH. The pHrodo dyes measure the intracellular pH in living cells; the lower the pH, the higher the fluorescence intensity.

Materials

- pHrodo AM variety Pack (Cat.no.P35380) [molecular probes]
- Intracellular pH Calibration Buffer Kit (Cat.no. P35379) [molecular probes]
- Ibidi 8 well slides

Procedure

Cells were grown ($1x10^4$ cells in 200µl) in 8-well ibidi slide till the desired confluency was reached. The pHrodo vial has to be thawed by room temperature before vortexing. 5 µL of the pHrodo dye have to be added to 50 µL of the PowerLoad concentrate, before pipetting into 5 mL of the Live Cell Imaging solution (LCIS).
The cells were washed with LCIS before the staining solution was added and incubated at 37 ° C for 30 minutes. After incubation time the dye solution was removed and fresh LCIS was added before analyzing the cells under the confocal microscope. To identify the pH in the lysosomes a Calibration kit was necessary. For the pH quantification a Valinomycin/ Nigericin stock solution was prepared which was described in the molecular probes protocol. The cell loading solution consists of the valinomycin/ nigericin stock solution and the desired pH calibration buffer (pH 4.5; pH 5.5; pH 6.5 and pH 7.5). After performing the desired cellular experiment with pH-sensitive pHrodo AM, cells are washed twice with LCIS before adding 10 µM of the Cell Loading Solution and incubating 5 minutes at 37°C. After incubation the cells are analyzed via confocal microscopy (LAS X 3.1.5.16308) at a fluorescence excitation and emission of 560/580 nm.

The cells were also analysed with the spectrometer after the preparation procedure. For this measurement the same setting as for the cathepsin assay was used: fluorescence intensity (FL), well scan read type (5, 1.125), shake off, and then bottom measurement at 40 ms using Perkin Elmer Microplates (black).

2.7.2 Lysotracker

The LysoTracker probes (Invitrogen/Molecular Probes) are used for labeling and tracking lysosomes in live cells. LysoTracker are fluorescent probes which accumulate in acidic organelles. The fluorescence dyes can be visualized at different wavelengths, so they are useful when multiple fluorescent colorants are used to mark cells simultaneously.

Materials

- Lysotracker Green DND-26 (Cat.no. L7526) [molecular probes]
- Hoechst 33258, pentahydrate (bis-benzimide) [molecular probes]
- Ibidi 8 well slides

Procedure

Cells were grown in 8-well slides till the desired confluency was reached.
The lysotracker vial has to be thawed by room temperature before centrifugation. After centrifugation step 1mM probe stock solution was diluted to a final working solution in growth medium. For the Lysotracker probe we chose a working concentration of 70 nM which was tested in previous experiments. The cells were incubated for 1 hour at 37°C with the Lysotracker dye. After staining the loading solution was replaced and the cells were washed twice with Live Cell Imaging solution (LCIS). For nucleus staining Hoechst was used with a final concentration of 2,5µg/ml (for 20 minutes). Before the slides were analyzed under the microscope the cells were washed again and LCIS was added. With some cells after the second staining a fixation was performed using 4% paraformaldehyde (incubate 10 minutes). Finally, the cells were analyzed via confocal microscopy (LAS X 3.1.5.16308) at a fluorescence excitation and emission of 504/511nm for the lysotracker and 350/461nm for the Hoechst dye.

3 Results

3.1 Alteration in lysosomal function

3.1.1 Cytotoxicity of T-DM1 in parental and resistance mamma carcinoma cells

For the cytotoxicity assay a MTT assay was performed and four parental cell lines and their resistance subclones were used: SKBR-3 cell line which over-expresses the HER2 targeting gene product, T38 where HER2 was artificially transfected into the original MDA-468 cell line, MDA-468 which is a classic triple negative cell line in which no HER2 is expressed and MCF-7 another negative control in which no ERBB2 gene amplification takes place.

The cytotoxicity assay was performed by using a T-DM1 dilution series from 0,001 µg/ml to 1000 µg/ml T-DM1. The MTT data was then analysed via GraphPad Prism software. From the MTT assay resulting dose response curve, the so-called EC50 value is calculated which represents the concentration of the tested agent that is required for 50% inhibition of the cell viability. Based on the dose response curve, it can also be observed how fast a substance acts on the cells. The dose-response curve (Figure 6) shows that the cell lines SKBR-3 and T38 differ from the control cell lines MDA-468 and MCF-7. The SKBR-3 cells start to decrease already at a T-DM1 concentration of 10^{-2} µg/ml. The T38 cells behave similar, in this cell line a concentration of 10^{-1} µg/ml T-DM1 is necessary to kill 50% of them. In the other two cell lines where no HER2 protein is overexpressed, much higher T-DM1 concentrations are needed. Focusing on the growth of the cells, it can be observed that the modified T38 cell line and their original cell line MDA-468 show a much faster proliferation which can be perceived very clearly in this experiment. In Table 10, all EC_{50} values were listed. The concentration is expressed in µg/ml. The T-DM1 cytotoxicity was also measured in the resistant cell lines of SKBR-3, T38 and MDA-468. Different resistant cell lines with different T-DM1 resistance levels were cultured, as expected the EC_{50} value increases with increasing resistance level compared to the mother cell line. In the T38 cell line, from a resistance level of 0.5 µg/ml T-DM1, an increase of the EC_{50} value can no longer be detected, which means that it

saturates, or a plateau occurs. In the MDA-468 resistance cells it can be observed that there is nearly no increase in the EC_{50} values in all three resistant cell lines.

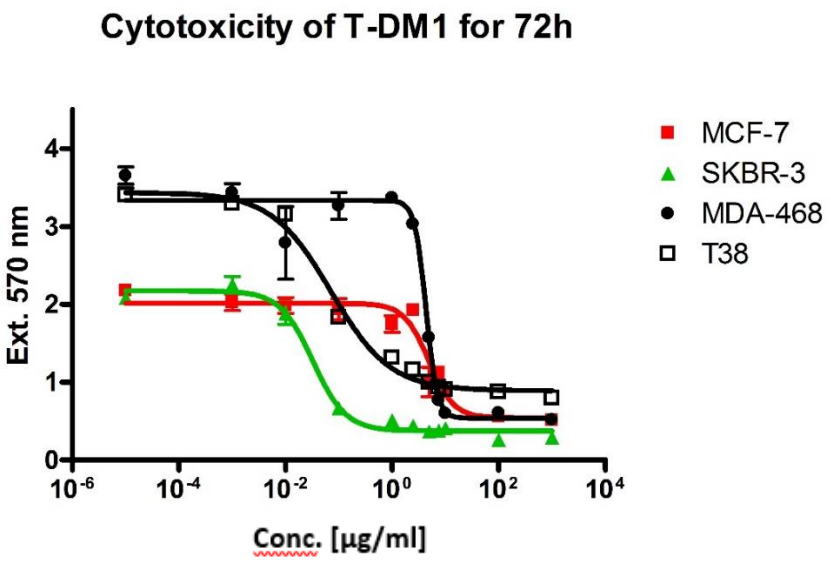

Figure 6 Dose response curve of the HER2 positive SKBR-3 cell line, T38 cell line where HER2 was artificially transfected and the two HER2 negative cell lines MDA-468 and MCF-7. The cells were exposed to T-DM1 for 72 hours.

Table 10 EC_{50} values of parental and resistance breast cancer cells after 72h T-DM1 exposure

cell lines	Mean EC_{50} [µg/ml]	S.D. EC_{50}
SKBR-3	0,03	0,018
SkBR-3 +0,003 µg/ml T-DM1	0,038	0,029
SkBR-3 +0,03 µg/ml T-DM1	6,985	0,478
SkBR-3 +0,3 µg/ml T-DM1	9,269	0,636
T38	0,08	0,029
T38 + 0,01 µg/ml T-DM1	2,742	0,059
T38 + 0,1 µg/ml T-DM1	5,779	0,938
T38 + 0,5 µg/ml T-DM1	9,838	1,86
T38 + 1 µg/ml T-DM1	9,609	3,571
MDA-468	4,447	0,534
MDA-468 + 0,5 µg/ml T-DM1	10,735	4,727
MDA-468 + 1 µg/ml T-DM1	10,138	4,784
MDA-468 + 1,5 µg/ml T-DM1	8,979	3,834
MCF-7	4,609	1,326

3.1.2 Cytotoxicity of Chloroquine in parental and resistance mamma carcinoma cells

Chloroquine, a substance which is also important in malaria treatment, was used to increase the pH value in the lysosomes to test the hypothesis that an alteration in lysosomal function leads to T-DM1 resistance. First, the toxicity of chloroquine in mamma carcinoma cells was determined (Figure 7). For this purpose, a chloroquine dilution series was performed from 0.001 µM to 1000 µM over a time period of 72 hours. As seen in the dose response curve below, all cell lines are eradicated between 10 and 100 µM chloroquine. From these results, the IC_{50}, IC_{25}, IC_{10} and IC_1 of chloroquine were calculated as starting point for incubations in combination with T-DM1. In parallel, we also pre-incubated cells over 24 h with chloroquine before 72 h incubation with T-DM1.

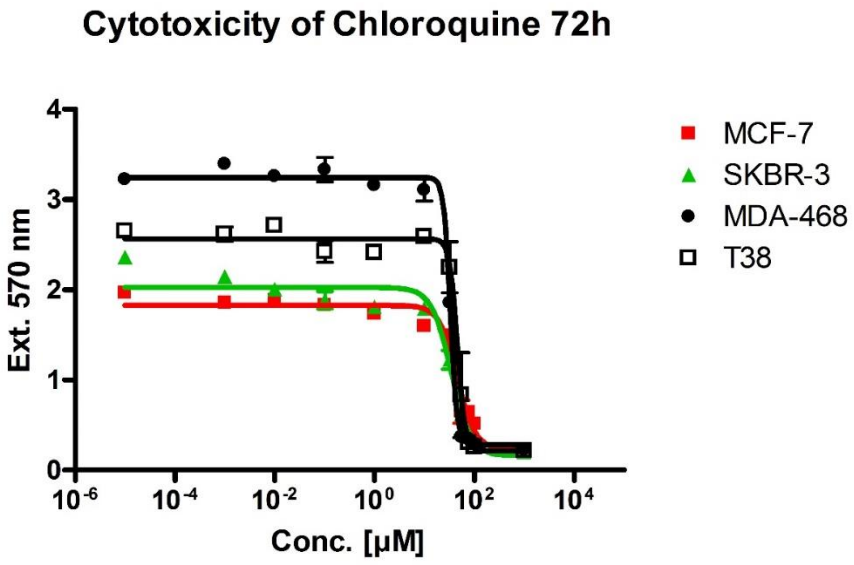

Figure 7 Dose response curve of the HER2 positive SKBR-3 cell line, T38 cell line where HER2 was artificially transfected and the two HER2 negative cell lines MDA-468 and MCF-7. The cells were exposed to Chloroquine for 72 hours.

Unfortunately, most of the experiments using a concentration above the IC_1 of chloroquine could not be evaluated because cell death started immediately. Also, the results in the experiments where chloroquine was pre-incubated for 24 h did not show any meaningful outcomes as the EC_{50} value did not change compared to the cytotoxicity test using only T-DM1. Therefore, only the results with a chloroquine concentration of IC_1 corresponding to a minimal toxic effect of chloroquine and the simultaneous incubation of chloroquine and T-DM1 over 72 h were used for the

evaluation and calculation of the resistance factor. The resistance factor was calculated as follows: The EC_{50} value of the cell line with chloroquine was divided by the EC_{50} value without chloroquine. In most cell lines, the addition of chloroquine made no difference in the T-DM1 resistance of the cells (Figure 8). The only exception is the sensitive cell line T38, which showed a significant increase in resistance after incubation with chloroquine by a factor fo 10.

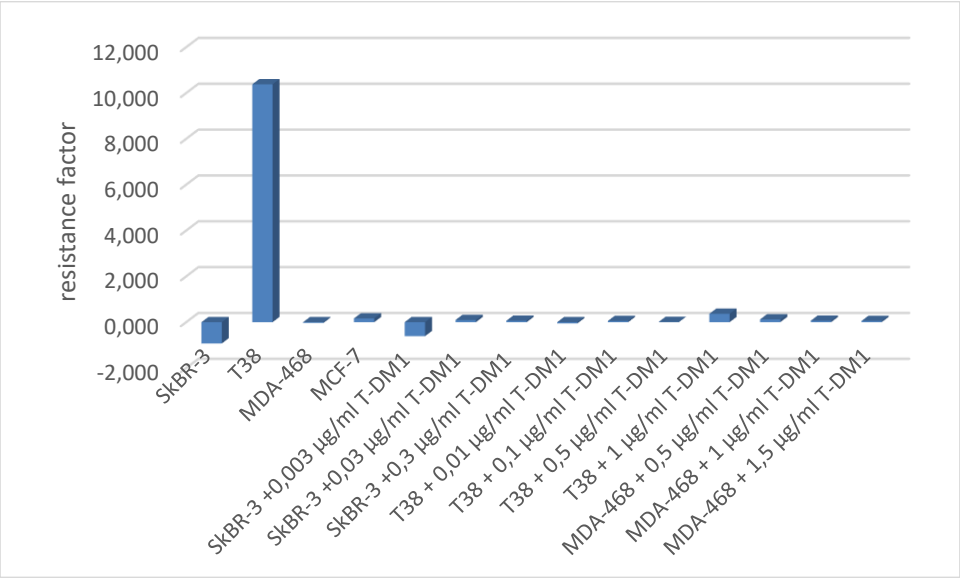

Figure 8 Resistance factor of sensitive mamma carcinoma cell lines and their resistance subclones. The resistance factor was calculated by the ratio of EC50 value of the cell line with chloroquine / EC50 value without chloroquine.

3.1.3 Lysosomal pH in sensitive cells vs. resistant cells

To check if our hypothesis is correct and the lysosomal pH increases in the resistant cell lines, an intracellular pH detection via pH_{rodo} dyes was performed. For this purpose, first a calibration series was carried out using special calibration buffers and examined under confocal microscopy (Figure 9, 10 and 11). Then all cells in the experiments were stained and the intensity of the dye was compared with the calibration images. In all investigated cell lines, the intensity of the staining was higher at a lower pH (corresponding to more acidic conditions in the lysosomes). At a pH of 7.5, there was only a faint lysosomal staining. As can be seen in the following pictures, the intensity decreases with increasing resistance level in all three cell lines. These results show that the lysosomal pH in the resistant subclones is changed compared to the original maternal line, and this change in lysosomal function may

have an effect on T-DM1 resistance. If we compare the three different sensitive cell lines, it can be found that SKBR-3 has a much higher pH (7.5) than MDA-468 and T38, which both have a pH between 5.5 and 6.5.
The pH fluctuations in the different cell lines were also measured via a fluorescence microplate reader. However, the results were very different and not reproducible, which means that a fluorescence microplate reader are not suitable for this kind of pH measurements. For this reason, these data cannot be shown or not included in the work.

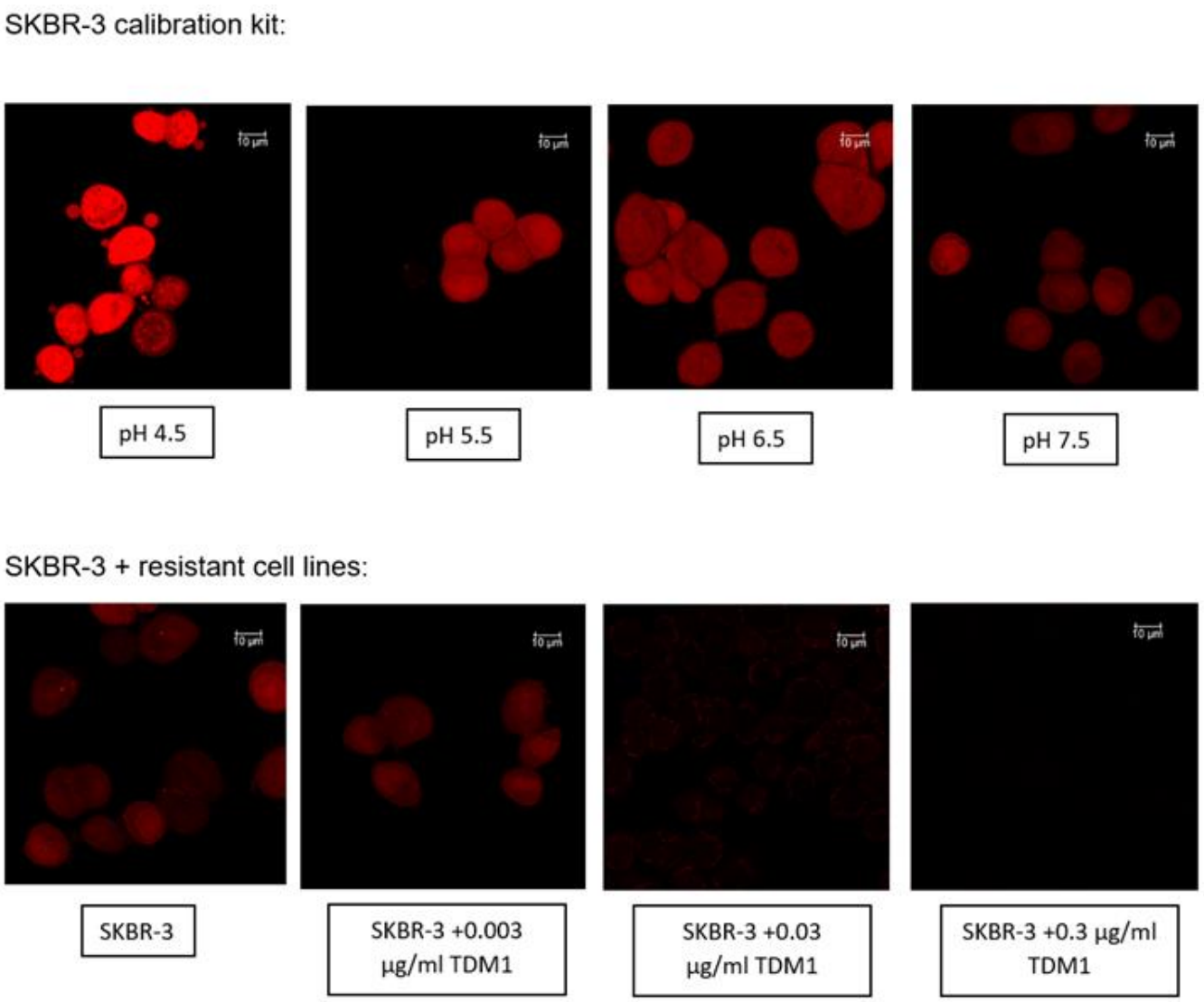

Figure 9 Intracellular pH Detection of SKBR-3 cell line and their resistant subclones via confocal microscopy.

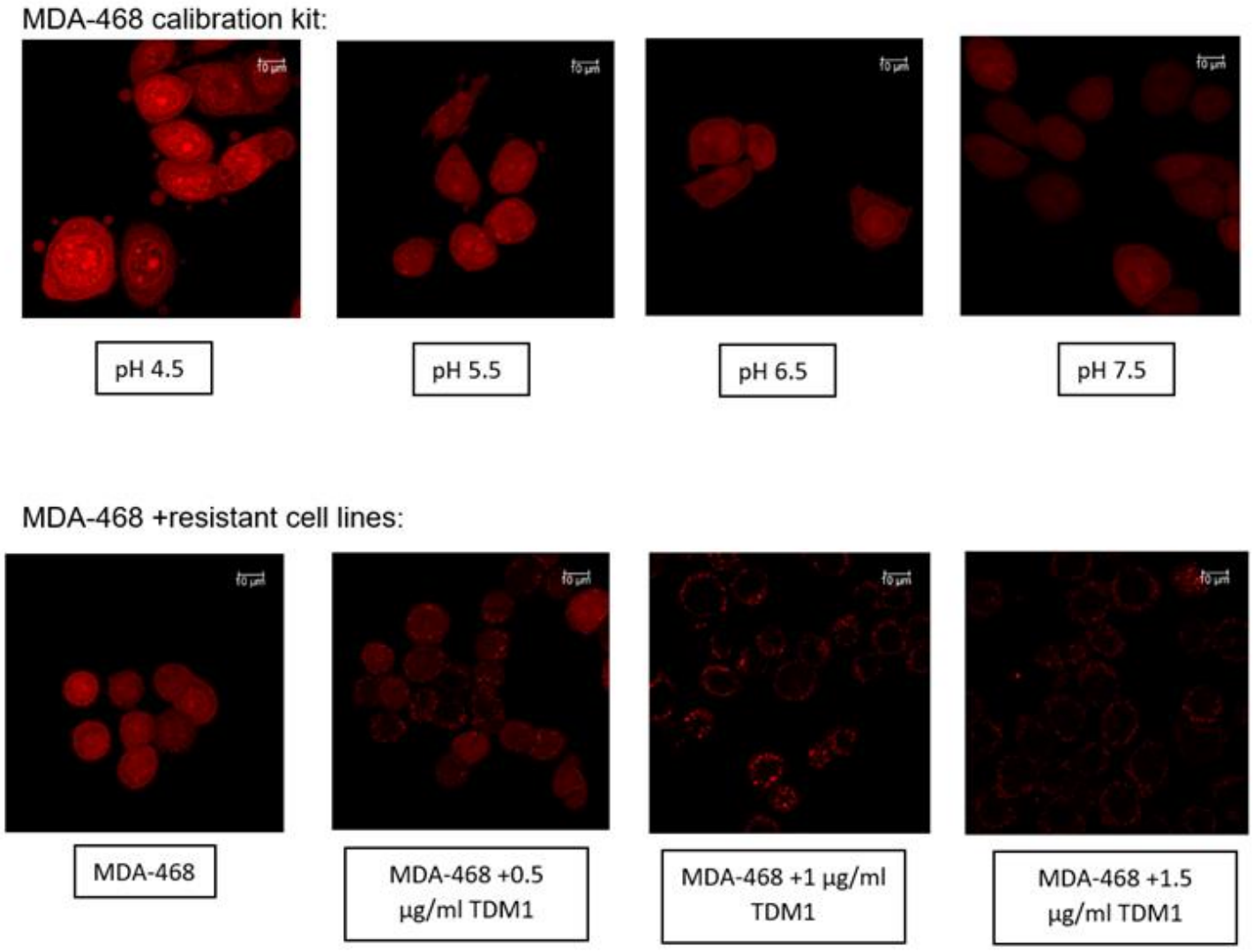

Figure 10 Intracellular pH Detection of MDA-468 cell line and their resistant subclones via confocal microscopy.

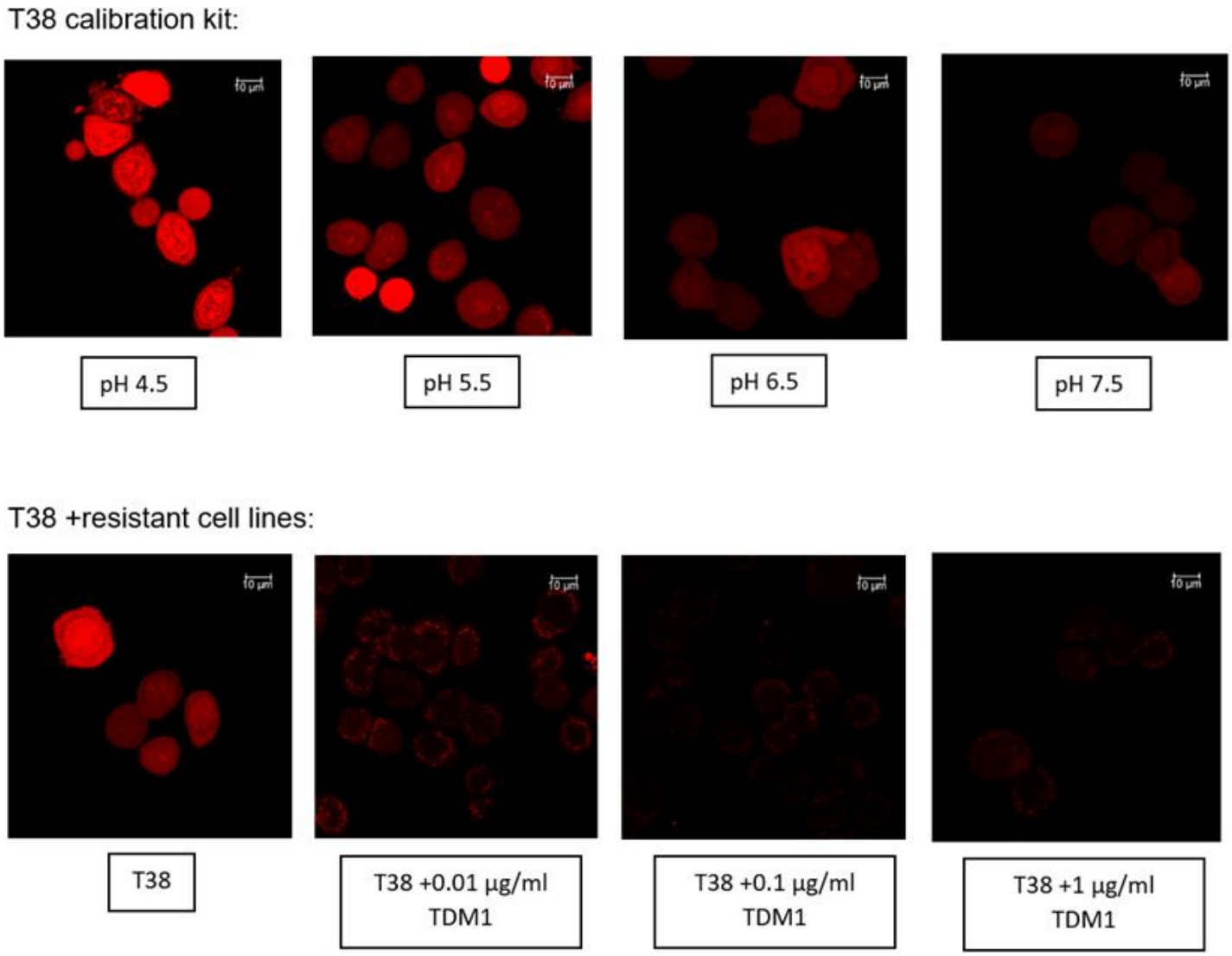

Figure 11 Intracellular pH Detection of T38 cell line and their resistant subclones via confocal microscopy.

3.1.4 Quantitative analysis of lysosomes in naïve and T-DM1 resistant cells

Many studies have already confirmed that cancer cells have a more acidic extracellular environment compared to normal cells. It is also proven that this environment has an influence on the size and number of lysosomes in those cells. For this reason, a quantitative analysis of the lysosomes in sensitive as well as in resistant cancer cells was performed. To investigate whether the size and the number of lysosomes change with increasing resistance level, a lysotracker dye was used. For a better presentation, besides the lysosomes, the cell nucleus was also colored via Hoechst. In Figure 12, the SKBR-3 and one SKBR-3 resistant cell line (SKBR-3 + 0.3 µg/ml TDM1) are presented. The lysosomes are stained green while the nucleus is stained blue. In the microscopy data no difference between the two cell lines can be determined. Therefore, a special software (Fiji image software) was used to evaluate the size and the number of the lysosomes.

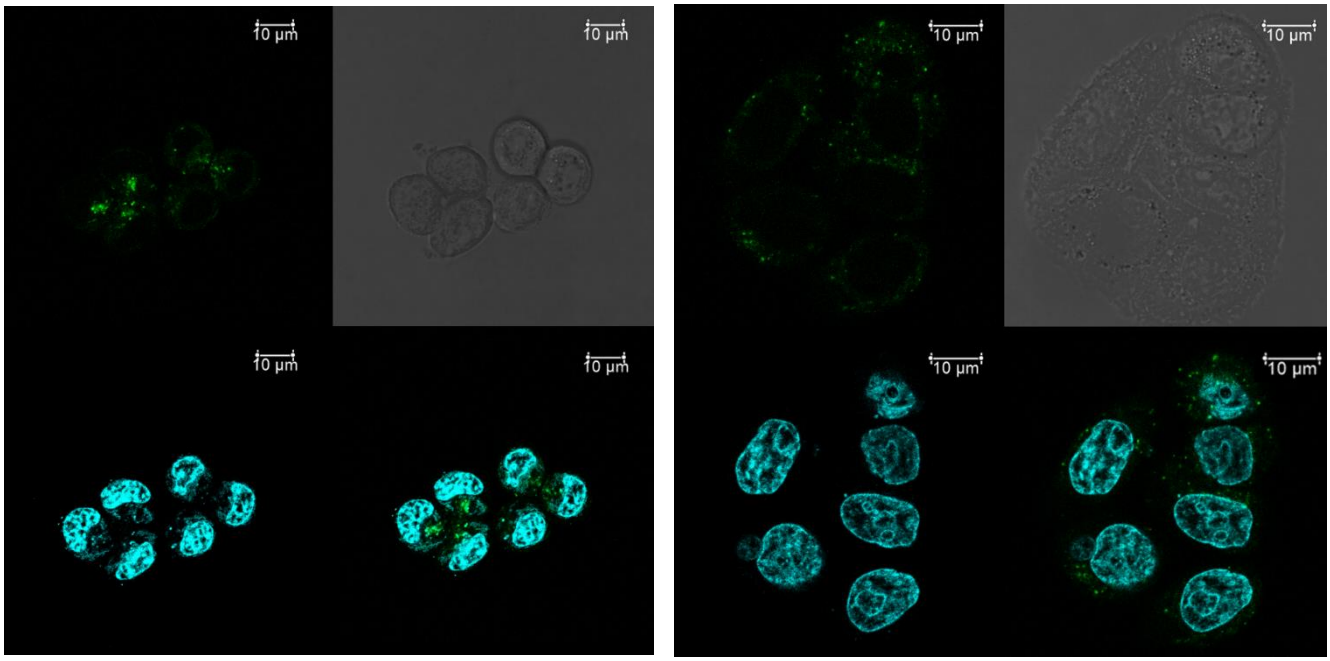

Figure 12 Immunofluorescence staining of lysosomes (green) and nuclei (blue) in HER2 positive breast cancer cells SKBR-3 (left) and their resistant subclone SKBR-3+ 0.3 µg/ml TDM1 (right) via confocal microscopy.

The fiji software is an open source image processing package based on ImageJ. After the confocal images could be evaluated by means of fiji software, it could be determined that the size of the lysosomes is not related to the resistance of the cells.

There was no difference in the size of the lysosomes. In all tested cell lines, approximately 97% of the lysosomes were below 100 nm in size. However, the quantitative analysis in lysosome count demonstrated differences between the cell lines (Figure 13). The number of lysosomes in resistant cell lines increased in comparison to the parent cell line in all three investigated models. Especially in the cell line MDA-468, a linear increase of lysosome count with the level of T-DM1 resistance was observed.

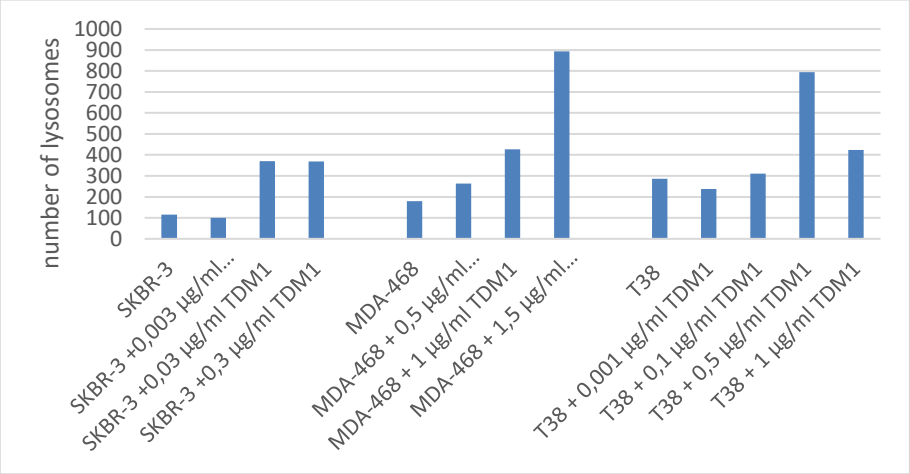

Figure 13 Quantitative analysis of the number of lysosomes in mamma carcinoma cell lines using Fiji software.

3.1.5 Validation of cathepsin expression

The enzyme activity could also have an important influence on the T-DM1 efficiency in the cells, which is why the cathepsin expression in the lysosomes was measured. The enzyme levels were quantified via fluorometer with a 328 nm excitation filter and 460 nm emission filter. First the lysate concentration had to be tested as well as the type of plate to be used. Via standard deviation and the variation coefficient the best option was determined which was a lysate volume of 25 µl and the black Perkin Elmer Microplate. In Figure 14, the results of the different plates and settings can be seen using the cell line SKBR-3 and MDA-468. The Perkin Elmer Microplate (black) and the Thermo Fisher Scientific plate Nunc A/S (white) were tested. The white plate could only be measured from above because the bottom is not transparent.

In the black plate it was noticeable that if we measure the fluorescence from the top the variation coefficient is four times as high as in the bottom measurement. The integration time makes no difference. But if we compare only the results from the top

measurements, a clear difference between the two plates could be observed. The relative fluorescence unit in the white plate is almost twice as high as in the black plate. The variability of measurements was independent of the integration time. According to this experiment, it can be stated that the measurement from below shows lower scattering and thus leads to the lowest standard deviation and variation coefficient. For further experiments black plates (PerkinElmer) are used and the cathepsin levels were measured from the bottom with 40 ms integration time.

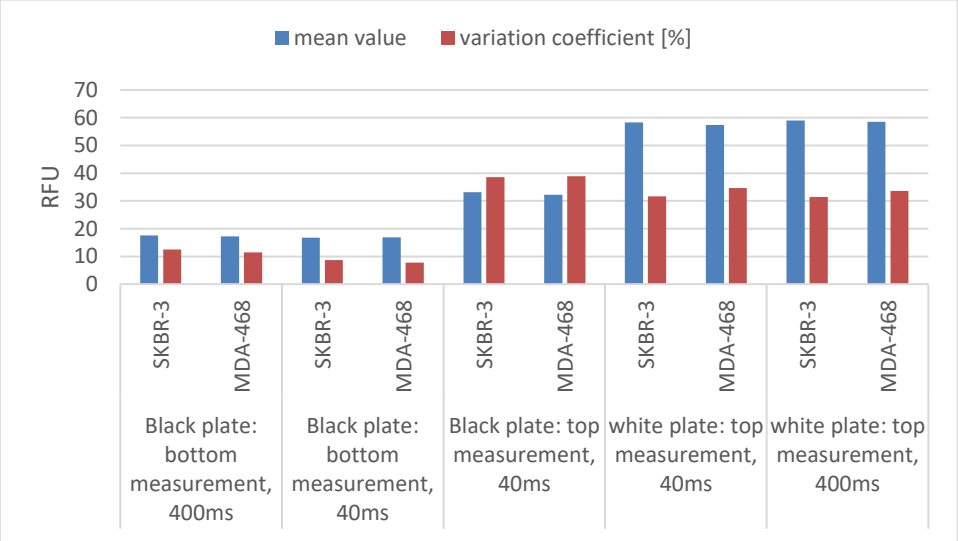

Figure 14 Pilot trial to figure out which are the best measurement settings and which plate should be used for further investigations.

After the measurement settings were established, the enzyme activity of lysosomal cathepsin D was analyzed using a cathepsin D assay. Based on the results, no significant difference in the cathepsin levels of the cell line SKBR-3 and MDA-468 with their resistant subclones could be found (Figure 15). The situation is different in the T38 cell line; in this cell line a significant increasing trend can be observed with rising resistance level. Additionally, a trend analysis was carried out by means of GraphPadPrism 4 and the outcome shows also a significant difference in the cathepsin expression of the resistant cells compared to the sensitive cell line.

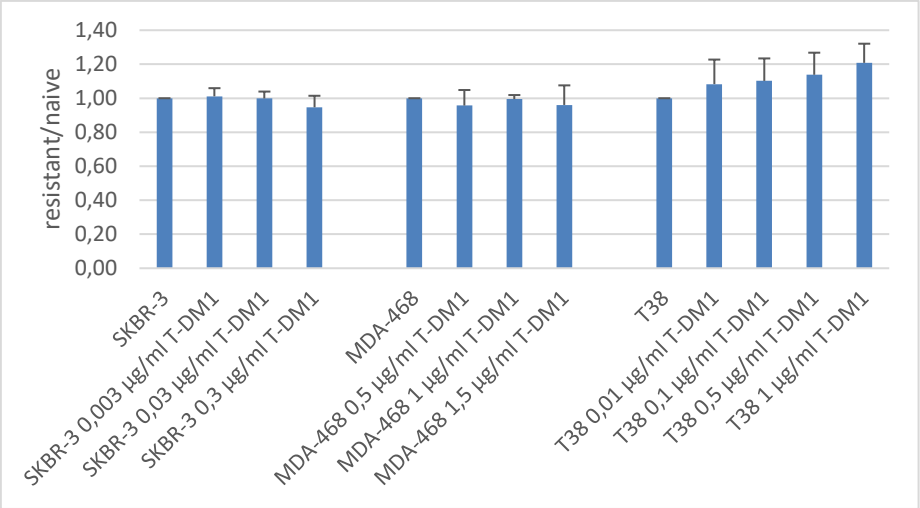

Figure 15 Expression of cathepsin D in SKBR-3, MDA-468 and T38 cell lines and their resistance subclones was measured via fluorometer with a 328 nm excitation filter and 460 nm emission filter.

Summary

To conclude the results of the lysosomal resistance mechanism, it could be proven that the pH in the lysosomes of the resistant cells changes. Resistant cell lines showed a significantly higher pH (above 7) than their original mother cell line thus confirming our hypothesis. Unfortunately, this could not be confirmed in cytotoxicity tests, where we tried to artificially increase the pH via chloroquine due to the inherent toxicity of the substance itself. Moreover, an increase in the lysosome count was detected in resistant cells strongly suggesting that T-DM1 resistance alters lysosome function and number. However, the cathepsin expression, the T-DM1 cleaving enzyme, showed little influence on the cell resistance.

3.2 CyclinB1/Cdk1 complex

3.2.1 Cell cycle distribution in sensitive and resistant cell lines

The cell cycle plays an important role in the efficacy of T-DM1, only in the M-phase of the cell cycle DM1 can bind to tubulin. Also, a defect in cell cycle regulation is suspected in resistant cells, therefore it is interesting to see if there are differences in the cell cycle distribution in sensitive and resistant cell lines. The proliferation assay was used to see how many cells are in the synthase phase and if there is a difference between the cell lines (Figure 16). The cell line with the lowest level of resistance shows the highest proliferation rate which was the case in all three cell lines. It is also striking that in the MDA-468 cell line the intermediary resistance level

(MDA-468+1 µg/ml TDM1) indicates the lowest proliferation compared to the other MDA-468 cell lines. If we compare these results with the population time of the cells, no connection could be recognized. Normally, we would assume that the cell line with the highest proliferation rate also has the lowest generation time. However, this could not be confirmed in our experiments.

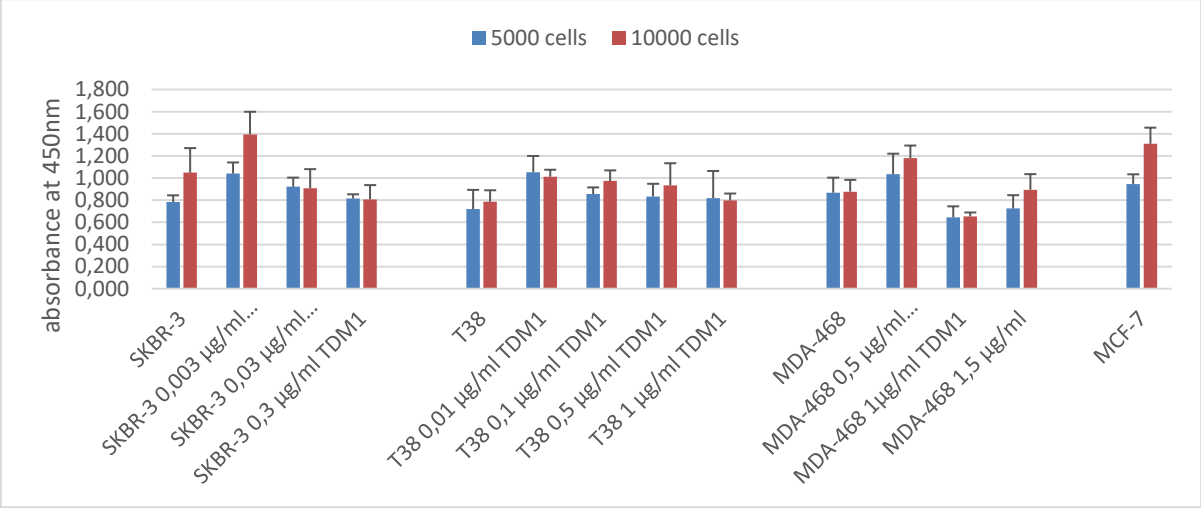

Figure 16 The action of T-DM1 resistance on cell cycle in SKBR-3, T38, MDA-468, MCF-7 cell lines and their resistant subclones. Cell cycle status was analysed using BrdU incorporation assay.

3.2.2 Connection between cyclinB1 expression and generation time of the cells

The generation time of the cells is the time required for the cells to double, so a low generation time means faster growth or proliferation of the cells. PDT results (Figure 17) show a reduction in doubling time in all intermediary and highly resistant cell lines, which means that they divide much faster than their sensitive mother cell line. The slightly resistant cells in the SKBR-3 and T38 cell lines show a slight increase in the generation time compared to the slightly resistant MDA-468 +0.5 µg/ml T-DM1 which only needs a few hours to divide. This experiment was carried out on the one hand with 3000 cells as well as 5000 cells and here it can be observed that in the experiment with fewer cells the doubling time is much lower compared to the experiment with 5000 cells.

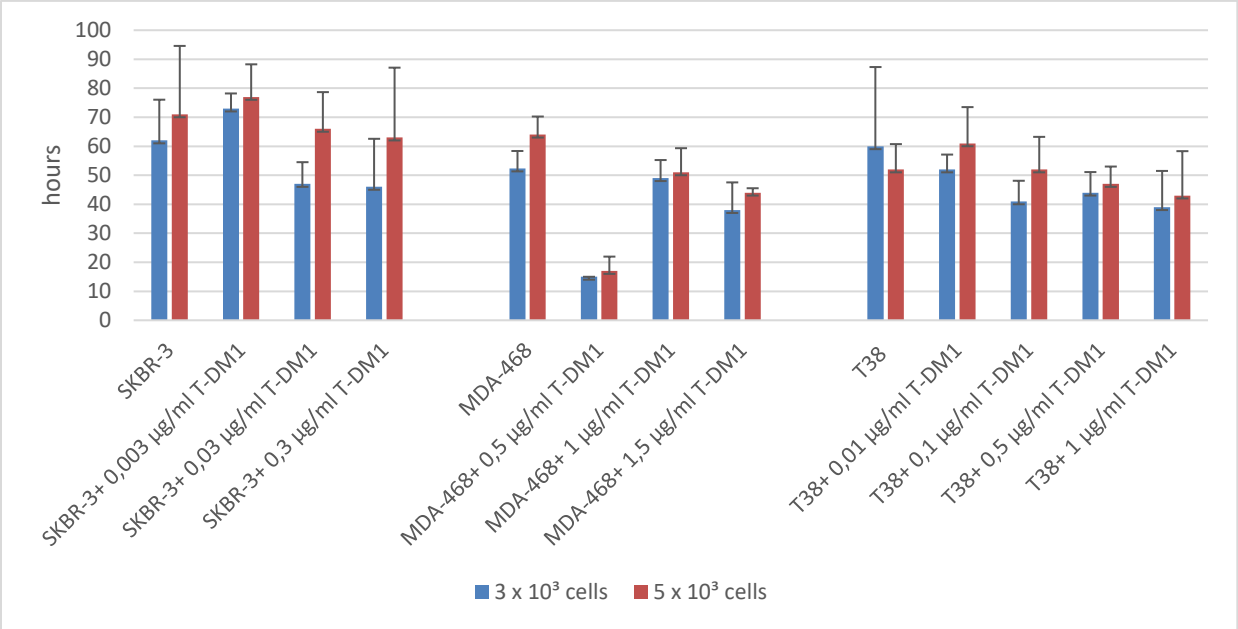

Figure 17 The doubling time in hours for each cell line, when 3000 cells (blue) and 5000 cells (red) were seeded.

Since cyclinB1 is the main regulator for the entry into the M phase, it is assumed that cyclinB1 is increased in cells with a low population doubling time. The cyclinB1 expression was measured via Western blot. As shown in the blots (Figure 18) below, cyclinB1 increases with growing resistance level. The same results were also obtained in the cell line T38 (data not shown). These results fit very well with the outcomes of the generation time of the cells. Resistant cells multiply faster the higher the resistance level and G2 / mitotic-specific cyclin-B1 which is a regulatory protein for mitosis increases as well. According to the literature, cyclinB1 forms a complex with Cdk1, this complex is responsible for the entry into the M-phase. Cdk1 was also analyzed by immunoblotting, but there were some problems in setting the right concentration and also the antibody binds very unspecific. Therefore, a representable blot could not be produced. However, it was possible to find out that there is no correlation between cyclinB1 and Cdk1. While cyclinB1 increases with increasing cell resistance, Cdk1 remains stable in most cells. As a positive control, GAPDH was used in all cells. It is a suitable loading control because of its stable and ubiquitous expression in our cellualr models.

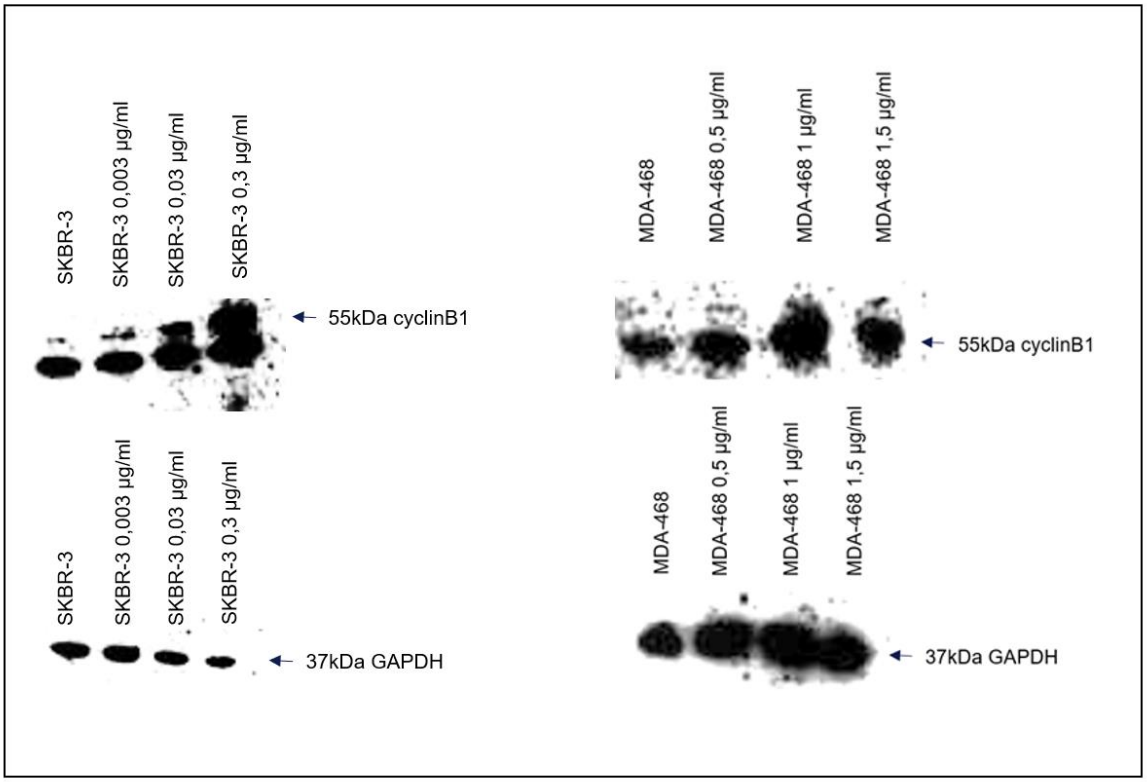

Figure 18 Immunoblot to detect the expression of CyclinB1 in SKBR-3 and MDA-468 cell lines and their resistant subclones. GAPDH was used as loading control for each blot.

We also started a trial to measure the FoxM1 expression in the cells (data not shown). FoxM1 is an oncogenic transcription factor which is overexpressed in a broad range of tumour types. Previously, it has been shown that high levels of FoxM1 in HER2 amplified mammary tumours could confer resistance to Herceptin or Taxol treatment. In our experiment, cyclinB1 increased with the resistance of the cells while FoxM1 was expressed the same in all cell lines. However, this experiment should be repeated several times to confirm the validity of its outcome.
Based on these findings, it is assumed that the cyclinB1 / Cdk1 complex has no direct influence on the resistance to T-DM1 and that FoxM1 is probably independent of cyclinB1.

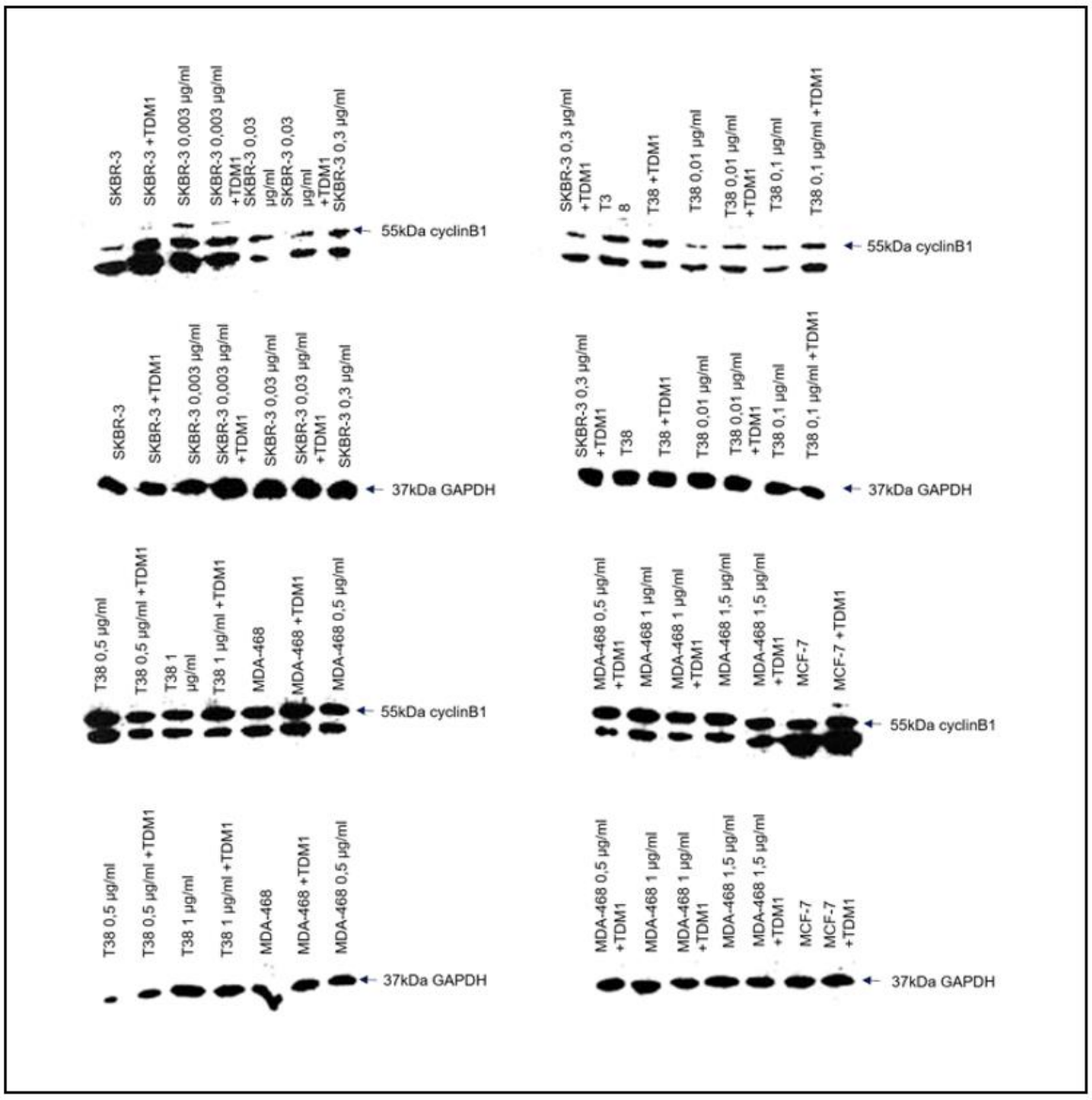

Figure 19 Effects of T-DM1 on cyclinB1 expression in different breast cancer models. T-DM1 is able to upregulate the expression of cyclinB1 in T-DM1 sensitive cancer cells but also in T-DM1 resistant cells. Cells were treated with T-DM1 (0,1 mg/ml) for 24 hours. Protein expression levels of cyclinB1 were evaluated by Western blot analysis using 10 mg of protein cell lysate. GAPDH was used as loading control for each blot.

We also analyzed the effects of T-DM1 on cyclinB1 activity. It has already been demonstrated in previous studies that in sensitive cell lines, T-DM1 leads to an accumulation of cyclinB1. In our experiment, this phenomenon could not only be observed in sensitive cell lines, but also in the resistant cells (Figure 19). The results showed a significant increase in cyclinB1 expression when the cells were 24 hours pre-incubated with T-DM1 (0.1 mg/ml) in both sensitive and trastuzumab emtasine-resistant cells.

3.2.3 Relative expression of cyclinB1, CdK1 and CdK2

Quantitative real time PCR was used to study the gene expression of cyclinB1, CdK1 and CdK2. For the experiment a cDNA dilution of 1:10 was used, because this concentration provided the most stable results. Cyclin-dependent kinase 2, known as cell division protein kinase 2, is highly similar to Cdk1 in humans. This protein kinase is important for entering the S phase and in this phase it forms a complex with cyclinA. The relative expression of CdK2 has also been compared with the BrdU incorporation assay to see if the cells which are mainly in the synthesis phase also have a higher Cdk2 expression, which was not the case. Also, no connection between Cdk2 and Cdk1 is apparent, which can be seen in Figure 20 and Figure 21.

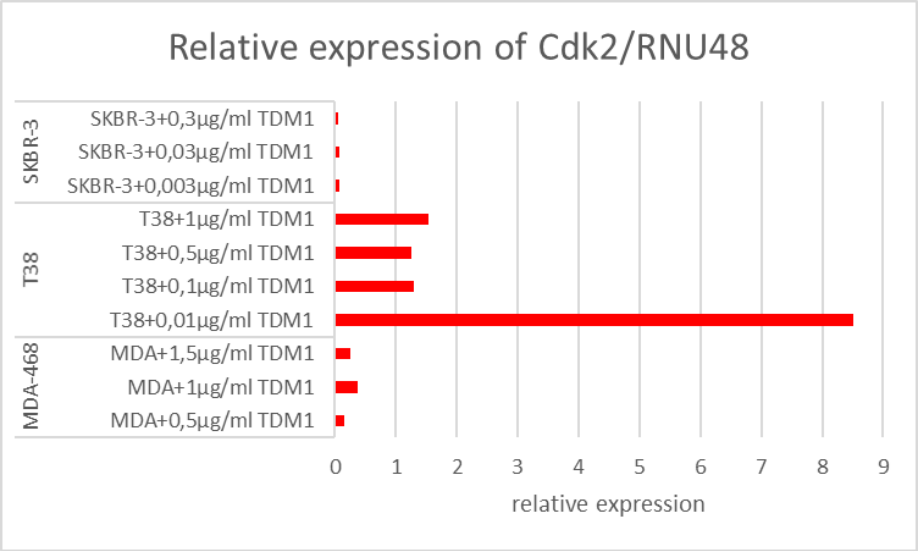

Figure 20 Relative gene expression of Cdk2/RNU48

Activation of cyclinB1/Cdk1 complex is crucial for the entry into mitosis and is regulated mainly by the expression of cyclinB1 protein. The relative expression of cyclin-dependent kinase 1 and cyclinB1 are very different so no trend can be recognized (Figure 21). Comparing the outcomes of the PCR with the immunoblots (Figure 17) only in the HER2 positive SKBR-3 cell line a match can be found, the PCR results show an increased cyclinB1 expression in resistant cells. However, the other two cell lines, MDA-468 and T38, indicate a slight reduction of cyclinB1 level with increasing resistance. Focusing mainly on the two cell lines MDA-468 and T38, it can be recognized that T38 has a decreased cyclinB1 expression related to MDA-468 cell line, which is interesting because the T38 cell line is originated from MDA-468 cell line.

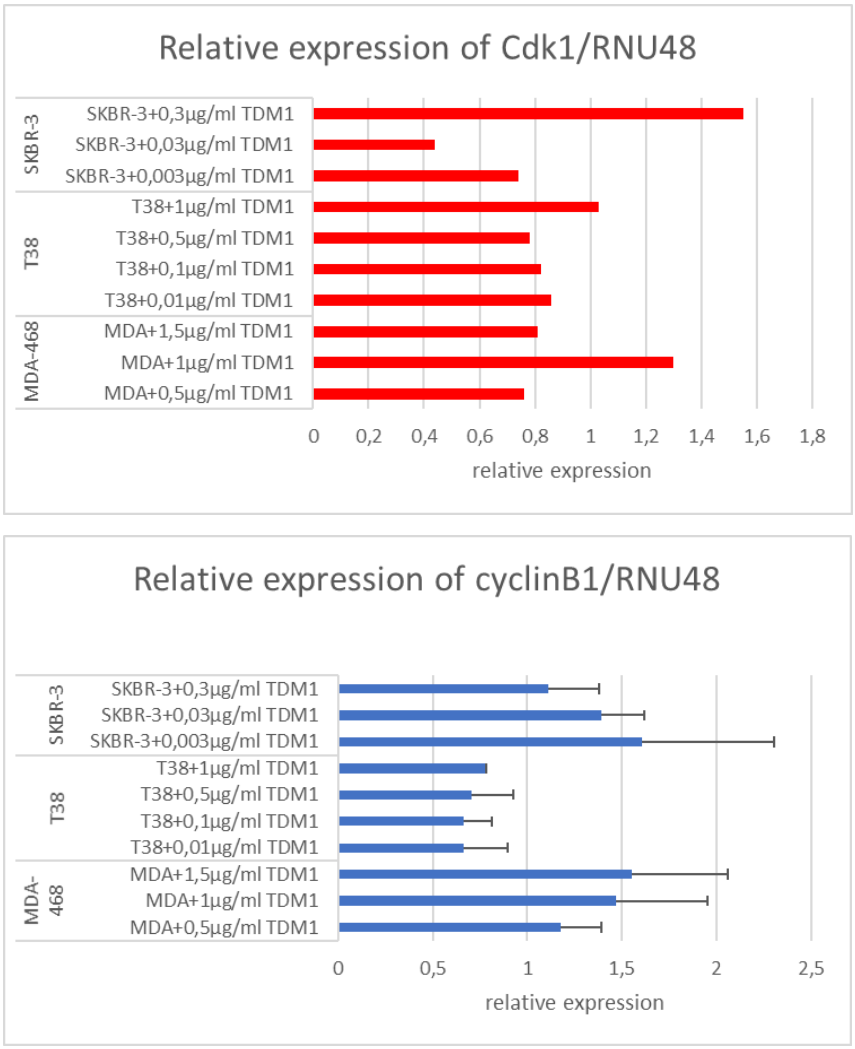

Figure 21 Relative gene expression of Cdk1/RNU48 and cyclinB1/RNU48

Summary

An aberrant cyclin B1/CdK1 complex as a possible T-DM1 resistance mechanism can largely be ruled out by our experiments. On the contrary, even an increase of cyclinB1 in resistant cell lines can be observed, which coincides with the faster generation times of resistant cells compared to their sensitive mother cell line. Also, T-DM1 has no impact on DNA synthesis as demonstrated by BrdU assays. Another interesting outcome is that cyclinB1 expression increased in both the sensitive and the resistant subclones after T-DM1 exposure.

4 Discussion

A central problem in oncology is the development of drug resistance. For this reason, it is important to try to uncover the resistance mechanisms in order to be able to overcome them in the next step. We started this work with the intention of identifying and describing resistance mechanisms against T-DM1. For this purpose, we used HER2 positive cell lines as well as HER2 negative and their resistant subclones for our experiments.

4.1 Alteration in lysosomal function

In the cytotoxicity assays, we have proven that the presence of the HER2 receptor is closely associated with the activity of T-DM1 (Figure 5). The EC_{50} of SKBR-3 and T38, which are HER2 overexpressing cell lines, are very low (0.030 µg/ml and 0.080 µg/ml) compared to MDA-468 and MCF-7 cell lines where the HER2 receptor is absent. T-DM1 shows also in MDA-468 and MCF-7 cell line a remaining activity at a certain concentration, which is probably triggered by unspecific uptake of the antibody conjugate. The unspecific uptake is probably the reason why trastuzumab emtansine leads to numerous side effects, as the monoclonal antibody-toxin complex is also taken up in non-cancerous cells which leads to cell death. Interestingly, the sensitivity of T38 is enhanced by a factor of 55 when compared with its original mother cell line MDA-468, which strongly indicates the determinant impact of the presence of the HER2 receptor independent of the original cellular background of MDA-468 (Mitri, Constantine, and Regan 2012).

In order to ensure an artificial increase in the pH value in the lysosomes, chloroquine was used. Chloroquine is a lysosomotropic agent that accumulates in acidic endosomal compartments, thereby affecting lysosomal enzyme activity by increasing the pH. This lysosomotropic agent shows strong fluctuations in the cell lines, in most trails a concentration of IC_{10} leads to complete cell death, therefore a Chloroquine concentration of IC_1 was used for further experiments (Piao and Amaravadi 2016). The first test where we pre-incubated chloroquine for 24 hours presented no meaningful results, probably because of the quick recovery of the mamma carcinoma cells, which is why no difference in the mode of action of T-DM1 could be observed. Interestingly, in the experiments where T-DM1 and Chloroquine were simultaneously

incubated with the cells for 72 hours, only in T38 cell line a significant increase in resistance was observed. This finding emphasises our hypothesis that a change in the pH in the lysosomes of T38 cell line contributes to the resistance mechanism of T-DM1. However, we would assume that this also happens in the other cell line where HER2 is overexpressed. However, exposure to chloroquine did not changethe EC_{50} of T-DM1 in the SKBR-3 cell line. These results suggest that the T38 cell line, where HER2 was artificially transfected, has a different signaling pathway than SKBR-3. In this so-called compensatory pathway, the lysosomal pH seems to play an essential role in T-DM1 treatment (Guha et al. 2015). In summary, an alteration in lysosomal pH in resistant breast cancer models could be determined due to the wide variability in the chloroquine results. To minimize these variances in further experiments, another substance should be used to change the pH in lysosomes artificially, where maybe a V-ATP pump inhibitor would be a good option.

The lysosomal pH in the parental as well as in the resistant subclones could be assessed quantitatively by optical comparison of confocal images, although there are some limitations within this method. As can be noticed in Figures 9, 10, 11 the lysosomes stainings in the resistant cells were only very weak or barely recognizable. It can thus be assumed that the pH in the resistant cells is higher than 7. Unfortunately, the calibration buffers only go up to pH 7.5, which is why above this value no measurements can be made. For time and cost reasons the experiment was carried out only once, but with each cell line several images were taken. In this experiment, the hypothesis that T-DM1 resistant cell lines have a higher pH than their sensitive cell line was indicated by our experiments. Virtually no dye is visible in the highly resistant cell lines, which means that the pH of the lysosomes is already in a slightly basic range. The cells stained with pH_{rodo} dyes were also measured via Spectramax. This alternative method using a fluorometric plate reader, however, was not successful due to the high variability of the signals. Thus, the fluorometric measurement were not suitable for this kind of analysis.

It is already known that cancer cells have an acid extracellular environment compared with normal cells, which also has an impact on the size and number of lysosomes. The quantitative lysosome analyses were performed via confocal microscopy and the evaluation was done with an imaging software called Fiji image.

The parental cell lines SKBR-3, T38, MDA-468 and MCF-7 as well as the resistance subclones showed no difference in size of the lysosomes. Therefore, it can be concluded that the size of the lysosomes has no direct influence on the resistance of the cells. However, the number of lysosomes in the resistant cells were increasing with increasing level of resistance to T-DM1. Interestingly, one would suspect that resistant cells possess fewer lysosomes than sensitive cell lines, since more lysosomes would point at a higher T-DM1 uptake into the lysosomes. In this case, T-DM1 would be cleaved into its single components, which would accumulate more drug in the cytosol. Hypothetically, this would then lead to a faster and more toxic effect of T-DM1. But, this does not seem to be the case, which in turn suggests that other factors are having an influence on the T-DM1 activity (Kato et al. 2013).

Cathepsins are lysosomal enzymes that are mainly responsible for the cleavage of trastuzumab from its toxic agent (DM1). As already mentioned, a slightly acidic pH is necessary for an optimal activity. According to our hypothesis, in the resistant cells a diminished cathepsin expression should be present whereby the cleavage of the individual components of T-DM1 is disturbed and so T-DM1 can no longer develop its full effect. In our case, we focused mainly on cathepsin D. However, no significant difference to the resistant cell lines was found in the cell lines SKBR-3 and MDA-468. The situation was different for the T38 cell line, where with increasing resistance levels the cathepsin content also increases slightly. This result is surprising because we assumed that the pH of the lysosomes increases with increasing resistance levels and therefore the cathepsin content should be decreasing. This again concerns the cell line T38, so we can assume that in this cell line where HER2 was artificially transfected maybe other signaling pathways or other resistance mechanisms take place (Fehrenbacher et al. 2005) (Lu et al. 2017).

4.2 Aberrant in CyclinB1/Cdk1 complex

Sabbaghi et al. reported that a defective cyclinB1/Cdk1 complex results in T-DM1 resistance. Theoretically, this should also be the case in our breast cancer models. We know that T-DM1 can only act in the M phase of the cell cycle and that the cyclinB1/Cdk1 complex is responsible for the progression into M phase. Since it is also known that cyclinB1 is crucial for the activation of this complex, one possible

explanation could be that cyclinB1 is reduced in the resistant cells and thus many cells pass into the M-phase barely or only very slowly. However, this assumption could be refuted by our experiments. In fact, the resistant cell lines proliferated faster than the parental cell lines (Figure 17). In addition, an increase in the cyclinB1 level could be detected in all resistant cells, which confirms that resistant breast carcinoma cells are more aggressive and robust and therefore divide much faster. Uncontrolled cell division is an indispensable event in tumour progression and is increasing in resistant cancer cells, which has already been confirmed through previous studies. The cyclinB1 expression also coincides with the results of the generation time, indicating that resistant cells have higher cyclinB1 expression, leading to faster division, which means that they are correlated with each other. Interestingly, the PCR analyses of cyclin B1 mRNA do not match the immunoblot results of cyclinB1 expression. In addition, the rate of DNA synthesis as assessed by the BrdU assay does not match the results of the generation times of the cells, where normally the cells with the highest proliferation rate should have the lowest doubling time. However, it must also be considered that the generation time refers to the entire cell cycle, which means that this is the time a cell needs to go through all four phases, while the proliferation rate represents only the S-phase. The cells also showed an increase of cyclinB1 after T-DM1 exposure, this phenomenon was observed in both the sensitive and the resistant cells. The reason can only be speculated and may be a cell response to the antibody drug conjugate. An explanation could be that they are trying to send as many cells as possible into the M-phase in order to increase the metabolic rate.
After the BrdU incorporation assay, the PDT assay and the Immunoblot analysis, a defect in the cyclinB1/Cdk1 complex as a possible T-DM1 resistance factor can be excluded.

In summary, the importance of identifying resistance mechanisms in cancer cells and characterizing them has led to a growing interest in scientific research. Over time, cancer under treatment becomes resistant. In order to counteract this, it is necessary to understand how resistance develops. Unfortunately, only a few resistance mechanisms have been fully researched and described so far. Therefore, it is essential to conduct further investigations to prevent or at least to be able to avoid treatment resistance in the future.

5 Literature

Aaltonen, K et al. 2009. “High Cyclin B1 Expression Is Associated with Poor Survival in Breast Cancer.” *British journal of cancer*.

Ballinger, Tarah, Jill Kremer, and Kathy Miller. 2016. “Triple Negative Breast Cancer—Review of Current and Emerging Therapeutic Strategies.” : 112–17.

Barok, Mark, Heikki Joensuu, and Jorma Isola. 2014. “Trastuzumab Emtansine : Mechanisms of Action and Drug Resistance.” 16(2): 1–12.

Choi, Hye Joung, Masayuki Fukui, and Bao Ting Zhu. 2011. “Role of Cyclin B1/Cdc2 up-Regulation in the Development of Mitotic Prometaphase Arrest in Human Breast Cancer Cells Treated with Nocodazole.” *PLoS ONE* 6(8).

Decallonne, B, and R Bouillon. 2003. “Ab r F.” 14(1): 33–43.

Juliette Sauveur, L Université Claude, Bernard Lyon, and Ecole Doctorale Ed. 2017. “Development and Characterization Od Models of Resistance to T-DM1 To Cite This Version : HAL Id : Tel-01449300 DEVELOPMENT AND CHARACTERIZATION OF MODELS OF RESISTANCE TO T-DM1.”

Eccles, Suzanne A. 2002. “The Role of C- Erb B-2 / HER2 / Neu in Breast Cancer Progression and Metastasis.” 6(4): 393–94.

Fehrenbacher, Nicole, Nicole Fehrenbacher, Marja Jäättelä, and Marja Jäättelä. 2005. “Lysosomes as Targets for Cancer Therapy.” *Cancer research* 65(8): 2993–95. http://www.ncbi.nlm.nih.gov/pubmed/15833821.

Fennelly, Colin, and Ravi K Amaravadi. 2017. “Lysosomes.” 1594: 293–308. http://link.springer.com/10.1007/978-1-4939-6934-0.

Filho, Rachid A El-aouar, Aurélie Nicolas, and Thiago L De Paula Castro. 2017. “Heterogeneous Family of Cyclomodulins : Smart Weapons That Allow Bacteria to Hijack the Eukaryotic Cell Cycle and Promote Infections.” 7(May): 1–17.

Gagliato, Debora de Melo, Denis Leonardo Fontes Jardim, Mario Sergio Pereira Marchesi, and Gabriel N. Hortobagyi. 2016. “Mechanisms of Resistance and Sensitivity to Anti-HER2 Therapies in HER2+ Breast Cancer.” *Oncotarget* 7(39). http://www.oncotarget.com/fulltext/7043.

Galanternik, Fernando, Enrique Díaz-cantón, Bernardo Amadeo Leone, and José Pablo Leone. 2016. “Novel Approaches to Target HER2-Positive Breast Cancer : Trastuzumab Emtansine.” : 57–65.

Garrett, Joan T., and Carlos L. Arteaga. 2011. “Resistance to HER2-Directed Antibodies and Tyrosine Kinase Inhibitors: Mechanisms and Clinical Implications.” *Cancer Biology and Therapy* 11(9): 793–800.

Glunde, Kristine et al. 2003. “Extracellular Acidification Alters Lysosomal Trafficking in Human Breast Cancer Cells.” *Neoplasia* 5(6): 533–45. http://linkinghub.elsevier.com/retrieve/pii/S1476558603800374.

Gogia, Ajay, and Jagdish Nigade. 2018. “Trastuzumab Emtansine : Antibody - Drug Conjugate in Treatment of Human Epidermal Growth Factor Receptor - 2 - Positive Metastatic Breast Cancer.” 2.

Horton, T et al. 2011. “MTT Cell Assay Protocol.” *Wallert and Provast Lab*.

Iqbal, Nida, and Naveed Iqbal. 2014. “Human Epidermal Growth Factor Receptor 2 (HER2) in Cancers : Overexpression and Therapeutic Implications.” 2014.

Jensen, EC. 2012. “The Basics of Western Blotting. Anat Rec (Hoboken).” *The anatomical record* 371: 369–71.

Kato, Yasumasa et al. 2013. “Acidic Extracellular Microenvironment and Cancer.” *Cancer Cell International* 13(1): 1. Cancer Cell International.

Kavallaris, Maria. 2010. “Microtubules and Resistance to Tubulin-Binding Agents.” *Nature Reviews Cancer* 10(3): 194–204.

Kocar, Muharrem et al. 2014. “P95-HER2 and Trastuzumab Resistance in Metastatic Breast Cancer ; Is Immunohistochemistry Appropriate ?” 19(1): 245–49.

Lapper, L E A H N K et al. 1999. “The ErbB-2 ⁻HER2 Oncoprotein of Human Carcinomas May Function Solely as a Shared Coreceptor for Multiple Stroma-Derived Growth Factors.” 96(April): 4995–5000.

Lavaud, Pernelle, and Fabrice Andre. 2014. “Strategies to Overcome Trastuzumab Resistance in HER2-Overexpressing Breast Cancers : Focus on New Data from Clinical Trials.”

Lindqvist, Arne, Wouter Van Zon, Christina Karlsson Rosenthal, and Rob M.F. Wolthuis. 2007. “Cyclin B1-Cdk1 Activation Continues after Centrosome Separation to Control Mitotic Progression.” *PLoS Biology*.

Lu, Shuyan et al. 2017. “Lysosomal Adaptation: How Cells Respond to Lysosomotropic Compounds.” *PLoS ONE* 12(3): 1–22. http://dx.doi.org/10.1371/journal.pone.0173771.

Sarah Morgan, B.S. and Jennifer R. Grandis, M.D.; 2010. “ErbB Receptors in the Biology and Pathology of the Aerodigestive Tract" NIH Public Access.” 315(4): 572–82.

Sonia Guha, Erin E. Coffey, Wennan Lu, Jason C. Lim, Jonathan M. Beckel, Alan M. Laties, Kathleen Boesze-Battaglia, and Claire H. Mitchell. 2015. “Approaches for detecting

lysosomal alkalinization and impaired degradation in fresh and cultured RPE cells: evidence for a role in retinal degenerations." Exp Eye Res

Martínez, María Teresa et al. 2016. "Treatment of HER2 Positive Advanced Breast Cancer with T-DM1: A Review of the Literature." *Critical Reviews in Oncology/Hematology* 97: 96–106.

Mitri, Zahi, Tina Constantine, and Ruth O Regan. 2012. "The HER2 Receptor in Breast Cancer : Pathophysiology , Clinical Use , and New Advances in Therapy." 2012.

Nahta, Rita, Mien-chie Hung, and Francisco J Esteva. 2004. "Advances in Brief The HER-2-Targeting Antibodies Trastuzumab and Pertuzumab Synergistically Inhibit the Survival of Breast Cancer Cells." (713): 2343–46.

Nonagase, Yoshikane, Kimio Yonesaka, Hisato Kawakami, and Satomi Watanabe. 2016. "Heregulin-Expressing HER2-Positive Breast and Gastric Cancer Exhibited Heterogeneous Susceptibility to the Anti-HER2 Agents Lapatinib , Trastuzumab and T-DM1." 7(51): 84860–71.

Peddi, Parvin F., and Sara A. Hurvitz. 2014. "Ado-Trastuzumab Emtansine (T-DM1) in Human Epidermal Growth Factor Receptor 2 (HER2)-Positive Metastatic Breast Cancer: Latest Evidence and Clinical Potential." *Therapeutic Advances in Medical Oncology* 6(5): 202–9.

Pfaffl, Michael W. 2004. "Relative Quantification." : 63–82.

Piao, Shengfu, and Ravi K. Amaravadi. 2016. "Targeting the Lysosome in Cancer." *Annals of the New York Academy of Sciences* 1371(1): 45–54.

Pohlmann, Paula R, Ingrid A Mayer, and Ray Mernaugh. 2009. "Resistance to Trastuzumab in Breast Cancer." 15(24): 7479–92.

Ríos-Luci, Carla et al. 2017. "Resistance to the Antibody–drug Conjugate T-DM1 Is Based in a Reduction in Lysosomal Proteolytic Activity." *Cancer Research* 77(17): 4639–51.

Roy, Suvra, and Vikash Kumar. 2014. "A Practical Approach on SDS PAGE for Separation of Protein." 3(8): 955–60.

Sabbaghi, Mohammad A. et al. 2017a. "Defective Cyclin B1 Induction in Trastuzumab-Emtansine (T-DM1) Acquired Resistance in HER2-Positive Breast Cancer." *Clinical Cancer Research* 23(22): 7006–19.

———. 2017b. "Defective Cyclin B1 Induction in Trastuzumab-Emtansine (T-DM1) Acquired Resistance in HER2-Positive Breast Cancer." *Clinical Cancer Research*.

Song, Yongmei et al. 2008. "Overexpression of Cyclin B1 in Human Esophageal Squamous Cell Carcinoma Cells Induces Tumor Cell Invasive Growth and Metastasis."

Carcinogenesis 29(2): 307–15.

Wen, X-f et al. 2006. "HER2 Signaling Modulates the Equilibrium between Pro- and Antiangiogenic Factors via Distinct Pathways : Implications for HER2-Targeted Antibody Therapy." (March): 6986–96.

6 Appendix

Table 11 Quantitative analysis of the number of lysosomes in parental and resistant cell lines using fiji imaging software.

cell lines	lysosomes/cell
SKBR-3	115
SKBR-3 +0,003 µg/ml TDM1	100
SKBR-3 +0,03 µg/ml TDM1	370
SKBR-3 +0,3 µg/ml TDM1	369
MDA-468	180
MDA-468 + 0,5 µg/ml TDM1	263
MDA-468 + 1 µg/ml TDM1	426
MDA-468 + 1,5 µg/ml TDM1	893
T38	286
T38 + 0,001 µg/ml TDM1	238
T38 + 0,1 µg/ml TDM1	311
T38 + 0,5 µg/ml TDM1	794
T38 + 1 µg/ml TDM1	423

Table 12 Expression of cathepsin D in SKBR-3, MDA-468 and T38 cell lines and their resistance subclones was measured via fluorometer with a 328 nm excitation filter and 460 nm emission filter.

cell lines	mean value	sdt deviation
SKBR-3	1,00	0,00
SKBR-3 0,003 µg/ml T-DM1	1,01	0,05
SKBR-3 0,03 µg/ml T-DM1	1,00	0,04
SKBR-3 0,3 µg/ml T-DM1	0,95	0,07
MDA-468	1,00	0,00
MDA-468 0,5 µg/ml T-DM1	0,96	0,09
MDA-468 1 µg/ml T-DM1	0,99	0,02
MDA-468 1,5 µg/ml T-DM1	0,96	0,12
T38	1,00	0,00
T38 0,01 µg/ml T-DM1	1,08	0,14
T38 0,1 µg/ml T-DM1	1,10	0,13
T38 0,5 µg/ml T-DM1	1,14	0,13
T38 1 µg/ml T-DM1	1,21	0,11

Table 13 BrdU incooperation assay. The action of T-DM1 resistance on cell cycle in SKBR-3, T38, MDA-468, MCF-7 cell lines and their resistant subclones.

	mean value	standard deviation	mean value	standard deviation
cell lines	5000 cells	5000 cells	10000 cells	10000 cells
SKBR-3	**0,784**	0,06	**1,049**	0,22
SKBR-3 0,003 µg/ml TDM1	**1,041**	0,10	**1,394**	0,21
SKBR-3 0,03 µg/ml TDM1	**0,922**	0,08	**0,907**	0,17
SKBR-3 0,3 µg/ml TDM1	**0,815**	0,04	**0,808**	0,13
T38	**0,719**	0,17	**0,786**	0,10
T38 0,01 µg/ml TDM1	**1,052**	0,15	**1,013**	0,06
T38 0,1 µg/ml TDM1	**0,856**	0,06	**0,974**	0,10
T38 0,5 µg/ml TDM1	**0,833**	0,12	**0,935**	0,20
T38 1 µg/ml TDM1	**0,818**	0,25	**0,797**	0,06
MDA-468	**0,868**	0,14	**0,877**	0,11
MDA-468 0,5 µg/ml TDM1	**1,036**	0,18	**1,179**	0,11
MDA-468 1µg/ml TDM1	**0,644**	0,10	**0,654**	0,04
MDA-468 1,5 µg/ml	**0,725**	0,12	**0,895**	0,14
MCF-7	**0,945**	0,09	**1,310**	0,15

Table 14 The doubling time in hours for each cell line, when 3000 cells (blue) and 5000 cells (red) were seeded.

cell lines	3 x 10^3 Zellen	standard deviation [%]	5 x 10^3 Zellen	standard deviation [%]
SKBR-3	**62**	14,05	**71**	23,59
SKBR-3+ 0,003 µg/ml T-DM1	**73**	5,20	**77**	11,24
SKBR-3+ 0,03 µg/ml T-DM1	**47**	7,51	**66**	12,66
SKBR-3+ 0,3 µg/ml T-DM1	**46**	16,56	**63**	24,09
MDA-468	**52**	6,03	**64**	6,24
MDA-468+ 0,5 µg/ml T-DM1	**15**	0	**17**	4,95
MDA-468+ 1 µg/ml T-DM1	**49**	6,24	**51**	8,33
MDA-468+ 1,5 µg/ml T-DM1	**38**	9,54	**44**	1,53
T38	**60**	27,30	**52**	8,74
T38+ 0,01 µg/ml T-DM1	**52**	5,13	**61**	12,49
T38+ 0,1 µg/ml T-DM1	**41**	7,09	**52**	11,24
T38+ 0,5 µg/ml T-DM1	**44**	7,09	**47**	6,00
T38+ 1 µg/ml T-DM1	**39**	12,49	**43**	15,31

Table 15 Relative gene expression of cyclinB1, CdK1 and Cdk2 normalized with RNU48.

cell lines	CyclinB1	Cdk1	Cdk2
MDA+0,5µg/ml TDM1	1,33	0,76	0,16
MDA+1µg/ml TDM1	1,13	1,3	0,38
MDA+1,5µg/ml TDM1	1,2	0,81	0,25
T38+0,01µg/ml TDM1	0,5	0,86	8,5
T38+0,1µg/ml TDM1	0,56	0,82	1,3
T38+0,5µg/ml TDM1	0,86	0,78	1,25
T38+1µg/ml TDM1	0,77	1,03	1,54
SKBR-3+0,003µg/ml TDM1	2,1	0,74	0,07
SKBR-3+0,03µg/ml TDM1	1,55	0,44	0,07
SKBR-3+0,3µg/ml TDM1	1,3	1,55	0,06

7 List of Figures

8 List of Tables